Biochimica et Biophysica Acta 1803 (2010) 72–94

Contents lists available at ScienceDirect

Biochimica et Biophysica Acta

journal homepage: www.elsevier.com/locate/bbamcr

Review

To bind zinc or not to bind zinc: An examination of innovative approaches to improved metalloproteinase inhibition

Jennifer A. Jacobsen, Jody L. Major Jourden, Melissa T. Miller, Seth M. Cohen *

Department of Chemistry and Biochemistry, University of California, San Diego, La Jolla, CA 92093-0358, USA

ARTICLE INFO

Article history:
Received 27 February 2009
Received in revised form 12 August 2009
Accepted 12 August 2009
Available online 25 August 2009

Keywords:
Zinc-binding group
Mechanism-based inhibitor
MMP

ABSTRACT

This short review highlights some recent advances in matrix metalloproteinase inhibitor (MMPi) design and development. Three distinct approaches to improved MMP inhibition are discussed: (1) the identification and investigation of novel zinc-binding groups (ZBGs), (2) the study of non-zinc-binding MMPi, and (3) mechanism-based MMPi that form covalent adducts with the protein. Each of these strategies is discussed and their respective advantages and remaining challenges are highlighted. The studies discussed here bode well for the development of ever more selective, potent, and well-tolerated MMPi for treating several important disease pathologies.

1. Introduction

Matrix metalloproteinases (MMPs) belong to a family of structurally related Zn^{2+}- and Ca^{2+}-dependent endopeptidases that are involved in the cleavage of extracellular matrix proteins. To date, over 20 MMPs have been identified and these enzymes can be loosely classified based on their substrate specificity into collagenases, gelatinases, stromelysins, membrane-type MMPs (MT-MMPs), and others (Table 1) [1,2]. In normal physiology, MMPs are required for various processes such as tissue remodeling, embryonic development, angiogenesis, cell adhesion and proliferation, and wound healing. MMPs are tightly regulated at both the transcriptional level and at the protein activation level [2–4]. Expression of MMP mRNA is generally low; however, transcript levels rise significantly in response to cytokines and growth factors during times of extracellular matrix remodeling [3,5]. After MMPs are synthesized, they are secreted as inactive zymogens and are found anchored to the cell surface or within the extracellular matrix [3]. Activation of MMPs then occurs through a variety of pathways, including proteolytic cleavage of the propeptide domain by other MMPs or by furin-like serine proteases [2,4]. MMP activity is constitutively regulated by endogenous protein inhibitors called tissue inhibitors of metalloproteinases (TIMPs). There are a total of four TIMPs (TIMP-1, -2, -3, and -4) and these four protein inhibitors are able to control the proteolytic activity of all MMPs [3,6–8].

Despite their physiological importance, misregulation of MMP activity leads to the progression of various pathologies such as arthritis, multiple sclerosis, periodontal disease, and cancer [4,9,10]. For example, in the case of cancer progression, the degradation of the extracellular matrix has linked MMPs to tumor development through metastasis and angiogenesis [9,11]. This has been shown with mouse models of cancer using MMP-knockout mice or mice that overexpress certain MMPs [11,12]. MMPs are not only expressed in tumor cells but are also expressed in the surrounding stromal cells that have been recruited to the neoplastic area, suggesting a broader role in cancer than just their matrix degrading abilities [9,13,14]. In addition to cancer, the expression of MMPs during the inflammatory response induced by hypoxia/ischemia leads to the breakdown of the blood–brain barrier (BBB) causing cell death and tissue damage [15]. The role of MMPs in other inflammatory ailments such as arthritis [16] and chronic obstructive pulmonary disease (COPD) [17,18] has further verified the importance of MMPs as a therapeutic target. Because of the role of MMPs in these pathologies, MMP inhibitors (MMPi) have emerged as an important area of drug development research.

By exploiting the presence of a metal ion and various substrate-binding pockets, numerous synthetic MMPi have been designed and developed over the past three decades [3,19–21]. The first generation of MMPi was small-molecule mimics of the natural peptide substrates of MMPs that were combined with a hydroxamic acid zinc-binding group (ZBG) to chelate the catalytic Zn^{2+} ion and inactivate the protein [19]. These were potent, broad-spectrum MMPi that were able to inhibit MMPs at low concentrations but without selectivity for one MMP over another. Batimastat (**1**, Fig. 1, Table 2) is an example of one of these early inhibitors. With the structure of more MMPs determined by crystallographic methods, second- and third-generation MMPi were no longer limited to substrate-like compounds and new inhibitors were designed with a variety of peptidomimetic and non-peptidomimetic structures. These next-generation compounds were

* Corresponding author.
E-mail address: scohen@ucsd.edu (S.M. Cohen).

0167-4889/$ – see front matter © 2009 Elsevier B.V. All rights reserved.
doi:10.1016/j.bbamcr.2009.08.006

Table 1
Classification of MMPs.

MMP family	MMP	Enzyme name
Collagenases	MMP-1	Collagenase-1, fibroblast Collagenase
	MMP-8	Collagenase-2, neutrophil Collagenase
	MMP-13	Collagenase-3
	MMP-18	Collagenase-4
Gelatinases	MMP-2	Gelatinase A
	MMP-9	Gelatinase B
Stromelysins	MMP-3	Stromelysin-1, Proteoglycanase
	MMP-10	Stromelysin-2
	MMP-11	Stromelysin-3
Membrane-type MMPs	MMP-14	MT1-MMP
	MMP-15	MT2-MMP
	MMP-16	MT3-MMP
	MMP-17	MT4-MMP
	MMP-24	MT5-MMP
	MMP-25	MT6-MMP
Other	MMP-7	Matrilysin-1, PUMP
	MMP-12	Macrophage metalloelastase
	MMP-19	RASI-1
	MMP-20	Enamelysin
	MMP-23	CA-MMP
	MMP-26	Matrilysin-2, endometase
	MMP-28	Epilysin

designed to achieve greater selectivity, with an IC_{50} value against the target MMP up to three orders of magnitude better (i.e., lower) than the IC_{50} values against all other non-target MMPs [22]. Prinomastat (**2**, Table 2) is one such example of a second-generation inhibitor with selectivity over MMP-1 and -7 [23]. These compounds were also developed to have an improved therapeutic index, a parameter that refers to the ratio between the concentration of inhibitor that causes toxicity versus the concentration needed for in vivo efficacy [24].

Even with improvements in the design of MMPi over the past few decades, therapeutic inhibition of MMPs has been challenging as evidenced by the fact that doxycycline, an antibiotic from the mid-20th century, remains the only FDA-approved MMPi [2,3,19,25,26]. One limitation of many MMPi is their use triggers dose-limiting musculoskeletal syndrome (MSS) as a side effect, which is characterized by joint stiffness, pain, inflammation, and tendinitis [9,25,27]. The observed MSS has been attributed to the poor specificity and, hence, broad inhibitory activity of early MMPi. In the past, MMP-1 inhibition was thought to be the cause of these side effects and this led to the development of MMP-1 sparing broad-spectrum inhibitors such as Prinomastat (**2**). However, Prinomastat still caused MSS in clinical trials [25]. Unfortunately, observations such as this, where preclinical findings are not maintained in more advanced trials, have plagued the field of MMPi development [9]. In a separate study, it was found that rats show signs of MSS when given broad-spectrum MMPi even though MMP-1 is absent from the rodent genome [27]. Therefore, it has been proposed that MSS may be caused by inhibition of another MMP, a combination of other MMPs, or by inhibition of other metalloenzymes [9,25].

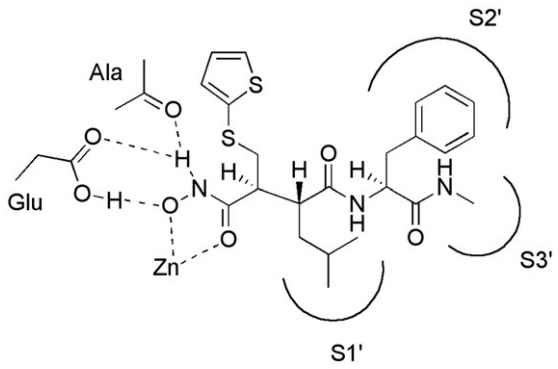

Fig. 1. Diagram of Batimastat (**1**) showing zinc-binding mode, hydrogen bonding, and distribution of substituents into the primed pockets [141].

As mentioned above, the inhibition of MMPs involved in normal matrix remodeling and of other metalloproteinases has been problematic [9,25,28]. For example, although the role of MMPs in the progression of cancer is well established, MMPs are also known to provide protective functions, such as repression of tumor angiogenesis and inactivation of metastasis-mediating chemokines [11]. Another factor that may have contributed to the problems of MMPi in clinical trials is the temporal dosing of these compounds [9,19]. The beneficial effects of MMPi in most preclinical trials have focused on early stages of cancer [9,19]. In contrast, most clinical trials administer MMPi in advanced stages of cancer, where their efficacy may be severely compromised. Similarly, in the case of MMPi for the treatment of stroke, evidence suggests that timing of drug administration is crucial [29,30]. MMPi administered in the first stages of stroke, immediately after the onset of reperfusion, show reduced breakdown of the blood–brain barrier (BBB) [30]. However, MMP inhibition at later stages showed no signs of reduced infarct size and an increase of neurological disorders due to interference with necessary tissue repair mediated by MMPs [30]. Continuing efforts to resolve the role of different MMPs as drug targets or anti-targets in various diseases, and the determination of the most beneficial stage of disease for MMPi administration, will be crucial for the success of MMPi.

The shortcomings of the first-generation MMPi prompted efforts to develop more specific MMPi [19]. This review focuses on recent developments in selective MMPi. Selectivity is a primary goal of MMPi design to improve efficacy and avoid unwanted side effects such as MSS. While the clinically relevant goal for MMPi specificity may be to achieve ~1000-fold difference in the relative affinity between MMPs, many current MMPi fall short of this goal. However, smaller differences in MMP affinity are discussed here to draw attention to structural features of MMPi that may lead to improved designs. While MMPi utilizing the traditional hydroxamic acid ZBG have shown improvements in selectivity as evidenced by compounds such as Prinomastat, the recurring side effects observed in clinical trials highlight the need for improved MMPi selectivity and new approaches to inhibition. In this article, a discussion of MMP structure, including substrate-binding pockets, is presented to aid in the discussion of recent MMPi developments. This is followed by an examination of three innovative approaches to MMP inhibition: (1) the use of potent ZBGs beyond the traditional hydroxamic acid group, (2) non-zinc-binding inhibitors, and (3) mechanism-based inhibitors that form covalent adducts with the protein. This short review only captures part of the efforts in the area of MMPi development; more comprehensive reviews of MMPi can be found in many excellent compilations from the recent literature [3,19–21].

2. Challenges of MMP structure for MMPi selectivity

Achieving selective inhibition of MMPs has proved a challenging goal because of the structural and functional similarity of most MMPs [31]. MMPs are multi-domain proteins with highly conserved signal, propeptide, and catalytic domains. The propeptide domain is composed of about 80 residues and contains a conserved "cysteine switch" motif PRCGXPD at the N-terminal, which binds to the catalytic Zn^{2+} ion to block its activity. The sulfhydryl group of the cysteine residue coordinates to the Zn^{2+} ion, thereby completing a 4-coordinate, tetrahedral coordination sphere and maintaining enzyme latency. MMP-2 and -9 contain three repeats of a fibronectin-like domain that are responsible for collagen recognition [32]. With the exception of MMP-7, -23, and -26, a haemopexin-like C-terminal domain is conserved among MMPs along with a hinge region of variable length linking the haemopexin domain to the catalytic domain [33,34]. In the case of MMP-23, the haemopexin repeat is replaced by an immunoglobulin-like domain along with a unique

Table 2
Structures and IC_{50} values of MMPi with a variety of ZBGs.

ID	Structure	IC_{50} values (μM) unless otherwise noted										Ref
		MMP-1	MMP-2	MMP-3	MMP-7	MMP-8	MMP-9	MMP-11	MMP-12	MMP-13	MMP-14	
1	Batimastat	3 nM	4 nM	20 nM		10 nM	10 nM					[141]
2	Prinomastat	8.3 nM*	0.05 nM*	0.3 nM*	54 nM*		0.26 nM*			0.03 nM*	0.33 nM*	[23]
3		9 nM										[45]
4	RS-104966	23 nM*								0.13 nM*		[46]
5		>400	0.135	0.081	1.1	0.042	>7			0.0018	5	[68]
6		>6		0.351	>22		1.3		0.002	0.120	1.1	[71]

7	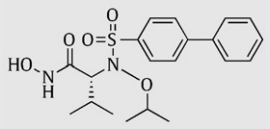	0.147	0.00009	0.050	>1	0.0016	0.0067		0.0098	[63]
8	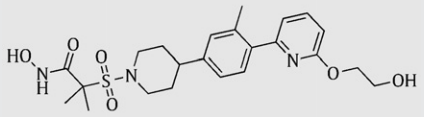	14	0.529	0.001			2.42		20.1	[65]
9	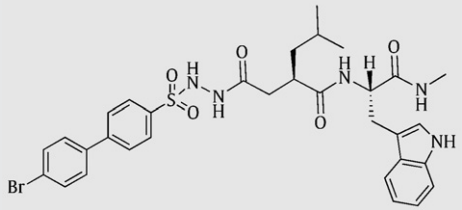	0.03	0.0098	1.7	0.475		0.003		17	[80]
10	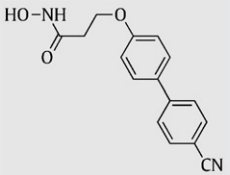	3.3	0.032	0.057						[81]
11	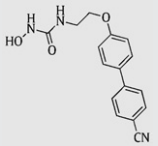	>50	>120	80		>120				[81,82]
12	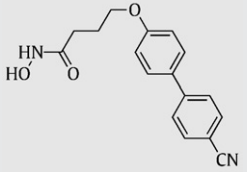			3.4						[82]

(continued on next page)

Table 2 (*continued*)

ID	Structure	IC_{50} values (μM) unless otherwise noted										Ref
		MMP-1	MMP-2	MMP-3	MMP-7	MMP-8	MMP-9	MMP-11	MMP-12	MMP-13	MMP-14	
13	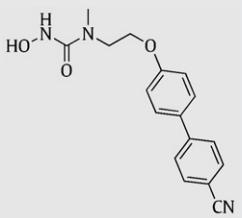		58	200		1200						[82]
14	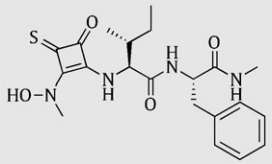	15										[84]
15	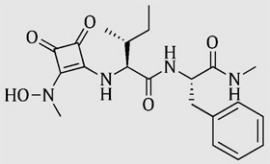	270										[84]
16	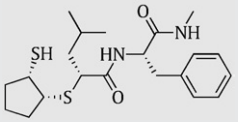	0.049*	0.0011*	0.470*	0.04*		0.00057*				0.024*	[85]
17	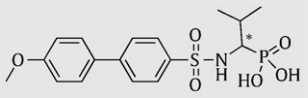		0.005* 1.2*	0.04* >100		0.0006* 0.7*						[87]

Top = *R* isomer
Bottom = *S* isomer

18	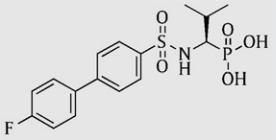	0.160	0.02	0.150	1.4	0.0011	0.059			0.013	0.032	[88]
19	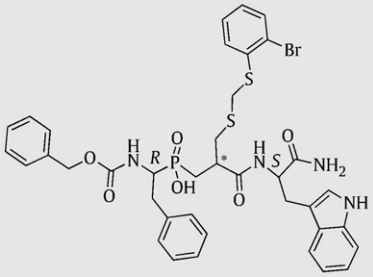		4.65*			18.4*	3.91*	0.11*		4.7*	30.1*	[92]
20	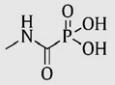	>100	0.02	90		20	>100					[94]
21	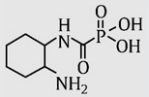	>100	4	>100		>100	20		>100	>100		[95]
22	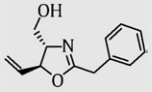	>500*	N/A				6*		N/A			[97]
23	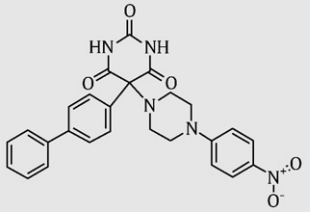	16	0.01	1.8		0.015	0.012				0.01	[98]

(continued on next page)

Table 2 (*continued*)

ID	Structure	IC_{50} values (μM) unless otherwise noted										Ref
		MMP-1	MMP-2	MMP-3	MMP-7	MMP-8	MMP-9	MMP-11	MMP-12	MMP-13	MMP-14	
24	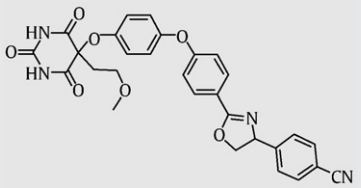		0.14			0.14			0.22	0.00036		[105]
25	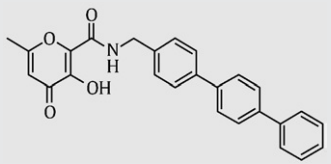	>50	>50	0.019								[76]
26	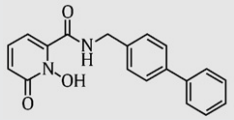	>50	0.92	0.56	>50	0.086	27.1		0.018	4.1		[75]
27	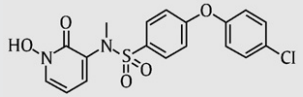	>1	0.005	0.056			0.0024			0.0025		[77]
28	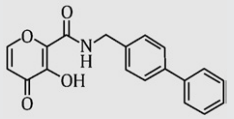	>50	4.4	0.077	>50	0.248	32.3		0.085	6.6		[75]

29	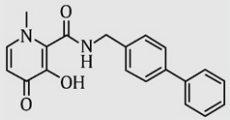	>50	16.5	41.7	>50	3.8	>50	1.2	16.5	[75]
30	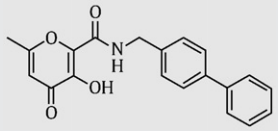	>50	9.3	0.24	>50	0.064	>50	0.022	20.6	[75,76]
31	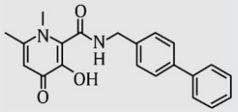	>50	7.6	>50	>50	5.0	>50	6.7	6.7	[75]
32	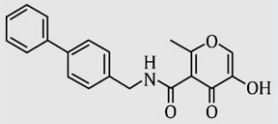	21% inhib. at 100 μM	34% inhib. at 100 μM	34% inhib. at 100 μM			33% inhib. at 100 μM			[109]
33	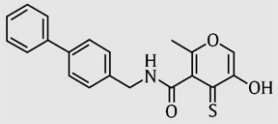	52% inhib. at 50 μM	23	45% inhib. at 50 μM			54% inhib. at 50 μM			[109]

N/A = not active up to solubility limit.
* = K_i value.

cysteine-rich domain [35]. MT-MMPs contain either a transmembrane domain and a cytoplasmic domain (MMP-14, -15, -16, and -24) or a glycosylphosphatidylinositol sequence (MMP-17 and -25) as a membrane anchor [6,36].

The conserved catalytic domain contains a catalytic Zn^{2+} ion, a structural Zn^{2+} ion, and one to three structural Ca^{2+} ions required for enzyme stability [4,31]. The catalytic Zn^{2+} ion is coordinated by three histidine residues in a conserved HEXGHXXGXXH motif and an axially coordinated water molecule responsible for substrate proteolysis in the active enzyme. The bound water molecule is additionally hydrogen bonded to the carboxylate group of a glutamic acid residue conserved in all MMPs [36]. The structural Zn^{2+} ion is bound by three histidine residues and one aspartic acid residue [37]. In addition, the catalytic domain contains a conserved methionine residue forming a "Met-turn" that forms a hydrophobic base around the catalytic Zn^{2+} ion [38,39].

The catalytic Zn^{2+} ion is flanked by "unprimed" (often referred to as the 'left-handed' side) and "primed" (often referred to as the 'right-handed' side) pockets designated S3, S2, and S1 and S1', S2', and S3', respectively. Of these pockets, the S1' pocket varies the most among the different MMPs in both the amino acid makeup and depth of the pocket, whereas the shallower S2' and S3' pockets are more solvent exposed [36]. MMPs can be generally classified based on the depth of the S1' pocket into shallow, intermediate, and deep pocket MMPs [36,40]. Shallow S1' pockets are found in MMP-1 and -7; MMP-2, -8, and -9 have intermediate S1' pockets while MMP-3, -11, -12, -13, and -14 have deep pockets [40–42]. Fig. 2 shows an example of each of these S1' pockets. These differences have been exploited in attempts to develop more selective MMPi with reasonable success. For example, since MMP-3 can accept a very large substituent in the S1' pocket (termed the P1' substituent), it can be targeted preferentially over MMP-1 and -7 by using large aromatic groups [31]. However, the use of bulky P1' substituents are merely a starting point for generating selectivity against a few MMP family members, and many of these inhibitors will also bind to intermediate and other deep pocket MMPs.

In the case of MMP-1 and -7, the S1' pocket is significantly occluded by Arg^{214} and Tyr^{214}, respectively, resulting in a much smaller pocket than that observed for other MMPs (Fig. 2). Successful targeting to the S1' pockets of MMP-1 and -7 has generally used smaller substituents such as leucine and isoleucine residues [43,44]. One such MMPi, **3** (Ro 31-4724, Fig. 3), is a potent inhibitor of MMP-1 [45]. Despite the shallow S1' pocket, there are several MMPi with large P1' substituents that have been reported as potent MMP-1 inhibitors [46,47]. For instance, the X-ray structure of MMP-1 complexed with an MMPi possessing a diphenylether sulfone P1' substituent (**4**) shows that the group extends deep into the S1' pocket, whereas the peptide-based inhibitor does not (Fig. 3). This is achieved through an induced fit mechanism where the Arg^{214} residue is displaced by inhibitor **4**, creating a larger, more accommodating substrate pocket, illustrating the importance of protein dynamics [46]. While MMP-7 also exhibits a smaller pocket due to occlusion by the analogous Tyr^{214}, an induced fit conformational change has not been observed for MMP-7 due to its shorter specificity loop creating a more rigid S1' pocket [31,43].

Intermediate S1' pockets are observed in MMP-8 as well as in the gelatinases MMP-2 and -9. Like MMP-1, MMP-8 belongs to the collagenase family and shares similar substrate specificity [48]. To accommodate the similar substrates with different pocket sizes, MMP-8 has a larger opening to the S1' pocket, formed by the Leu^{160} and Ala^{161} residues, than observed for MMP-1 [36]. The catalytic domains of MMP-2 and MMP-9 are highly homologous with hydrophobic S1' pockets described as tunnels leading toward the solvent [48,49]. The main structural differences between these two enzymes are seen in residues 425–431 of MMP-9, which form a loop in the S1' pocket that is not observed in MMP-2 [49]. Variability in size and shape of the S1' pocket is due to the orientation of the residues Thr^{426} and Arg^{424} of MMP-2 and -9, respectively, located at the bottom of the pocket [49]. Structures of MMP-9 co-crystallized with different MMPi reveal that the Arg^{424} residue is highly flexible and with some MMPi can move into a position that blocks the S1' pocket [50]. The occlusion by the Arg^{424} residue explains why some MMPi with long P1' substituents do not inhibit MMP-9 as well as they inhibit MMP-2 [50]. Due to the small differences in the S1' cavity, achieving MMPi selectivity between the gelatinases MMP-2 and -9 is a significant challenge. One strategy to overcome these similarities is to target additional pockets, including the S2 and S3' sites, where variability between the gelatinases is more pronounced [36,51,52].

The S1' specificity pockets of MMP-3, -11, -12, -13, and -14 are generally characterized as being large and open channels. In comparison to other MMPs, the S1' loop of MMP-12 most closely resembles that of MMP-8 due to the presence of similar helical turns at the bottom of the loop. However, the MMP-8 S1' pocket is closed off by Arg^{214}, whereas the MMP-12 pocket is open and extends to the solvent surface [53]. Of the large pocket MMPs, MMP-12 is unique in that it can accommodate binding of polar groups due to the Thr^{215} residue within the S1' pocket where generally a Val or Ala residue is present in other MMPs [48,53]. The large hydrophobic S1' pocket of MMP-13 has a highly flexible "S1' specificity loop" consisting of residues 245–253, which has been shown to play a role in the binding of large P1' substituents (vide infra) [46]. X-ray crystal structures show flexibility in the S1' loop, even in the presence of inhibitor binding, as evidenced by missing electron density [41,46] and confirmed by NMR spectroscopy [54]. This pocket is highlighted by the Leu^{218} residue, which lies to the side of the pocket creating an open space. In contrast, the equivalent residue in MMP-1, Arg^{214}, occludes the S1' pocket creating a shallow binding pocket (vide supra).

The rough classification of S1' specificity pockets into shallow, intermediate, and deep pockets can aid in the development of selective MMPi. However, the flexibility of these pockets is important to consider in the design of new compounds for targeting a given MMP. One such example is MMP-1, which has a shallow specificity pocket but can accommodate a diphenylether backbone in **4** commonly used to target intermediate and deep pocket MMPs. Further structure analysis through X-ray crystallography and NMR spectroscopy with inhibitors showing high selectivity will advance this area of study.

3. 'To bind zinc': improvement of the ZBG in search of selective MMPi

3.1. Early ZBGs

The design of MMPi has traditionally involved the use of a ZBG due to the fact that the mechanism by which MMPs cleave their substrates directly involves the catalytic Zn^{2+} ion [55–57]. Upon binding of the substrate, the zinc-bound water molecule attacks the substrate carbonyl carbon, and the transfer of protons through a conserved Glu residue to the amide nitrogen of the scissile bond results in peptide cleavage [32,56,57]. Therefore, ZBGs in MMPi serve to displace the zinc-bound water molecule and inactivate the enzyme [19]. In addition, the ZBG acts as an anchor to lock the MMPi in the active site and direct the backbone of the inhibitor into the target substrate-binding pockets.

Early MMPi typically included use of one of several ZBGs, including hydroxamic acids, carboxylates, thiols, and phosphonic acids [32]. Of these, hydroxamic acids emerged as the preferred chelator for Zn^{2+} proteases due to their relative ease of synthesis and potent binding [21,58–60]. Hydroxamic acids are monoanionic, bidentate chelators that bind a variety of metal ions including Zn^{2+}. A contributing factor to the effectiveness of hydroxamates is the hydrogen bonding that results between the heteroatoms of the ZBG and neighboring amino acid residues that are conserved in all MMP active sites (Fig. 1).

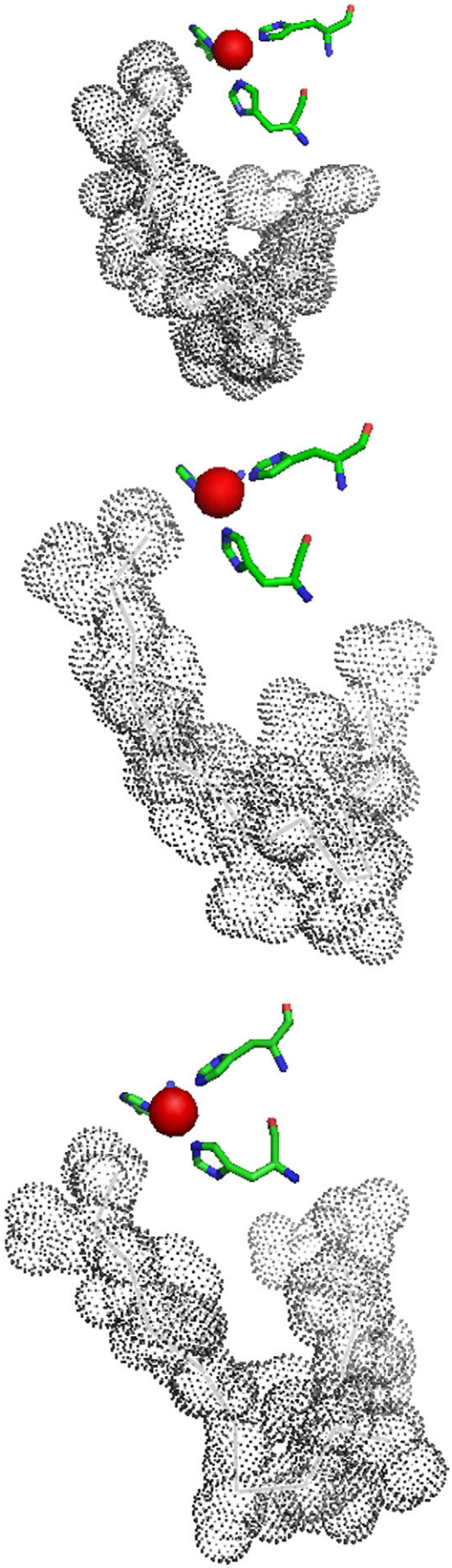

Specifically, the NH group and deprotonated OH group of the hydroxamic acid ZBG form hydrogen bonds with Ala and Glu residues, respectively [19].

There has been some concern that the use of strong chelators, such as hydroxamic acids, as ZBGs may preclude the development of selective MMPi [19,20,22] due to undesired activity against off-target metalloenzymes [25]. Despite this concern, several hydroxamate- and carboxylate-based MMPi have been reported that show good selectivity between different MMPs [61–65]. Additionally, a recent study involving a macrophage cell model that monitored the activities of several metalloenzymes including COX (heme iron dependent), iNOS (non-heme iron dependent), TACE (zinc dependent), and MMPs (zinc dependent) in the presence of various MMPi demonstrated that the mere presence of a strong chelator as part of an inhibitor did not inherently produce off-target metalloenzyme inhibition. Furthermore, this cell-based study showed that the off-target activity of a given ZBG did not necessarily reflect the off-target activity of an inhibitor containing the same ZBG [66].

Though potent inhibitors of MMPs, no hydroxamate-based MMPi have been approved by the FDA. Many hydroxamate MMPi have shown adverse musculoskeletal side effects in clinical trials presumably caused by inhibition of other metalloproteins [21,25,26]. However, the generally poor oral bioavailability may be another factor limiting the efficacy of hydroxamic acids [2,19,25,26]. Furthermore, the hydroxamic acid functional group can be metabolized via dehydroxylation or it may be cleaved by exopeptidases to release hydroxylamine [2,67]. This decreases the effective concentration of the hydroxamate-based inhibitor and reduces its in vivo potency.

Despite the aforementioned problems associated with hydroxamic acids and the low potency of some carboxylate inhibitors, investigations continue on inhibitors containing both of these well-established ZBGs. Recently, the main focus of research has been toward the development of inhibitors with increased selectivity for a single MMP. With this goal in mind, Wyeth published a series of biphenyl sulfonamide carboxylate MMPi in 2005 that were designed for the treatment of osteoarthritis and have remarkable selectivity for MMP-13 [68–70]. In order to gain selectivity over MMP-2, which is highly homologous to MMP-13, the P1' substituent was extended to take advantage of the steric limitations of the shorter S1' loop of MMP-2. As an example, compound **5** was a potent inhibitor of MMP-13 (IC_{50} = 1.8 nM) [68]; reasonably selective over MMP-2 (IC_{50} = 135 nM), MMP-3 (IC_{50} = 81 nM), and MMP-8 (IC_{50} = 42 nM); and highly selective over MMP-1 (IC_{50} > 400 μM), MMP-7 (IC_{50} = 1.1 μM), MMP-9 (IC_{50} > 7 μM), and MMP-14 (IC_{50} = 5 μM) [68]. Compound **5** exhibits 100% bioavailability when dosed orally in rats at 20 mg/kg and displays >50% inhibition of cartilage degradation in bovine cartilage explant at 10 ng/mL [68].

Wyeth used this carboxylic acid scaffold as a starting point to develop MMP-12 selective inhibitors for the treatment of COPD, in which MMP-12 has been suggested to be a viable target for therapeutic intervention [17,18]. In 2009, a series of inhibitors with improved selectivity towards MMP-12 over MMP-13 were generated by using a fused ring system [71]. Rather than increasing the length of the P1' substituent, which would favor targeting MMP-13, it was found that restricting the rotation of the biphenyl group favored binding in the less flexible MMP-12 S1' pocket. Inhibitor **6** demonstrated 60-fold selectivity for MMP-12 over MMP-13 and was additionally reported to be selective over MMP-1, -3, -7, -9, and -14. This inhibitor demonstrated in vivo efficacy in an MMP-12-induced

Fig. 2. Surface dot representations of the S1' specificity loops for MMP-7 (top, PDB code 1MMQ, shallow pocket), MMP-8 (middle, PDB code 1ZP5, intermediate pocket), and MMP-3 (bottom, PDB code 1CIZ, deep pocket). The catalytic Zn^{2+} ion is represented as a red sphere and the coordinating histidine residues are highlighted in green.

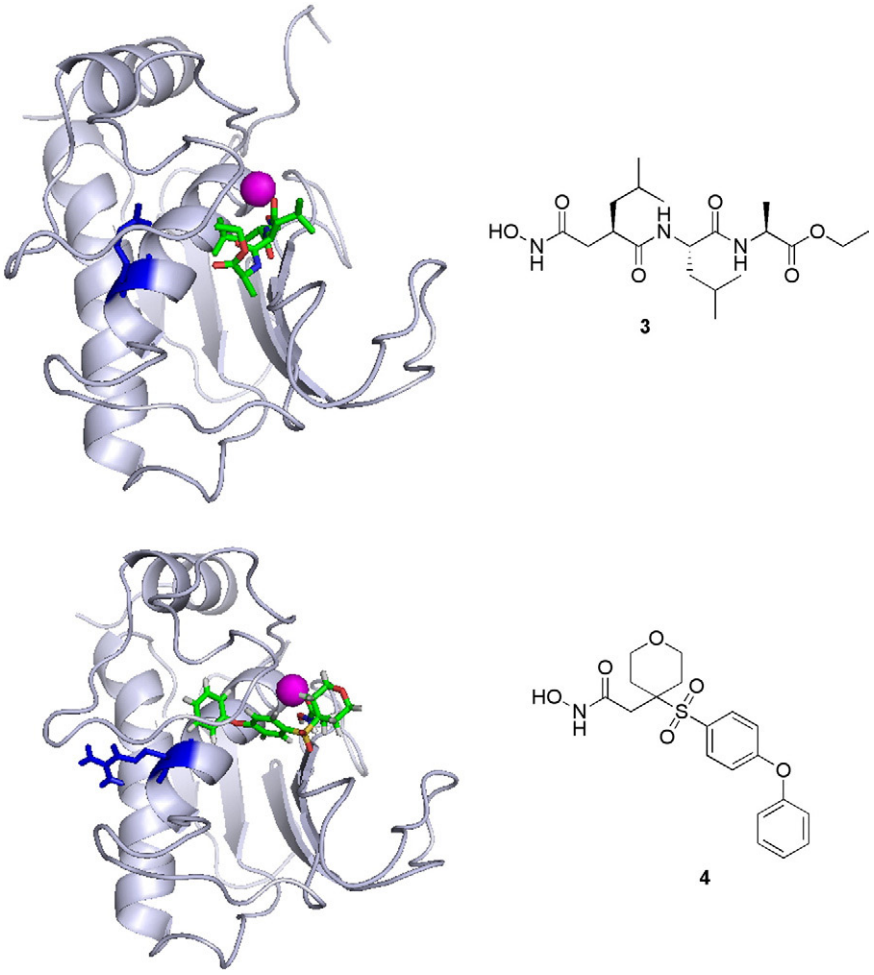

Fig. 3. Top. Ribbon drawing of MMP-1 (grey) complexed with the peptide-based inhibitor Ro 31-4724 (**3**) (green) showing occlusion of the S1' pocket by the arginine residue (highlighted in blue) (PDB code 2TCL) [45]. Bottom. Ribbon drawing of MMP-1 (grey) complexed with the diphenylether sulfone inhibitor RS-104966 (**4**) (green) showing displacement of the arginine residue (highlighted in blue), allowing for penetration of the inhibitor into the S1' pocket (PDB code 966C) [46]. The catalytic Zn^{2+} ion is represented as a purple sphere in both views.

mouse model of pulmonary inflammation. The minimum oral dose of **6** for efficacy in this model was 5 mg/kg two times a day.

Several selective hydroxamate inhibitors have been developed in recent years. Rossello et al. have developed selective hydroxamic acid inhibitors of MMP-2 as potent anti-angiogenic agents [63]. The addition of alkyl substituents at the carbon atom adjacent to the hydroxamic acid added lipophilic interactions with the S1 region of the active site and improved the selectivity towards MMP-2. Inhibitor **7** represents one of the most selective MMP-2 inhibitors of this series (>18-fold over MMP-8, -9, and -14 and >500-fold over MMP-1, -3, and -7) [63]. Compound **7** was evaluated with a HUVEC (human umbilical vein endothelial cells) chemoinvasion test and, at 1 μM, was shown to reduce invasion across a Matrigel barrier to a basal level. Another example of a selective hydroxamate inhibitor was a compound designed with specificity towards MMP-3 for the treatment of chronic non-healing wounds [65]. This compound (**8**) inhibits MMP-3 with an IC_{50} of 1 nM and is >500-fold selective over MMP-1, -2, -9, and -14. To achieve this selectivity, inhibitor **8** uses a reverse sulfonamide group in which the sulfur and nitrogen have been reversed in their placement with respect to the hydroxamic acid binding group. This adds steric bulk near the hydroxamic acid, which favors the large opening of the S1' pocket in MMP-3.

It is clear that hydroxamate and carboxylate ZBGs can be developed into highly selective MMPi through careful consideration of inhibitor backbones for targeting the substrate pockets of individual MMPs. The inhibitors discussed have been devised by taking advantage of a growing body of MMP crystallographic studies, in combination with computer modeling, to attain greater selectivity for the S1' pocket than their substrate analogue predecessors. In particular, specific inhibitors for MMP-13 have been designed with elongated backbones to probe deep into the S1' pocket, while rigid backbones have been found to improve targeting of MMP-12. In addition, emphasis on the opening of the S1' pocket, rather than the interior of the pocket, has helped in the development of MMP-3 selective inhibitors. Though many inhibitors with hydroxamate or carboxylate ZBGs continue to be investigated, a number of alternative ZBGs have also been developed as a possible means to improving selectivity, bioavailability, and pharmacokinetics.

Investigation of novel ZBGs has become an important aspect of MMPi development. Fig. 4 displays a multitude of ZBGs (**ZBG1**–**34**) that have been recently described in the literature. These include oxygen, nitrogen, and sulfur donor–atom ligands and include monodentate, bidentate, and tridentate chelators. This variety of ZBGs displays a wide range of affinities for the active site Zn^{2+} ion and provides new opportunities to orient an inhibitor in the active site. As mentioned before, early ZBGs include hydroxamic acids (**ZBG1**), carboxylic acids (**ZBG2**), thiols, and phosphorus-based ZBGs. For ease of reference, ZBGs that have some similarities to these early zinc-binding groups are discussed first. This is followed by an examination of a newer class of nitrogen-based ZBGs. Finally, a discussion of the heterocyclic bidentate chelators will be provided [72–78].

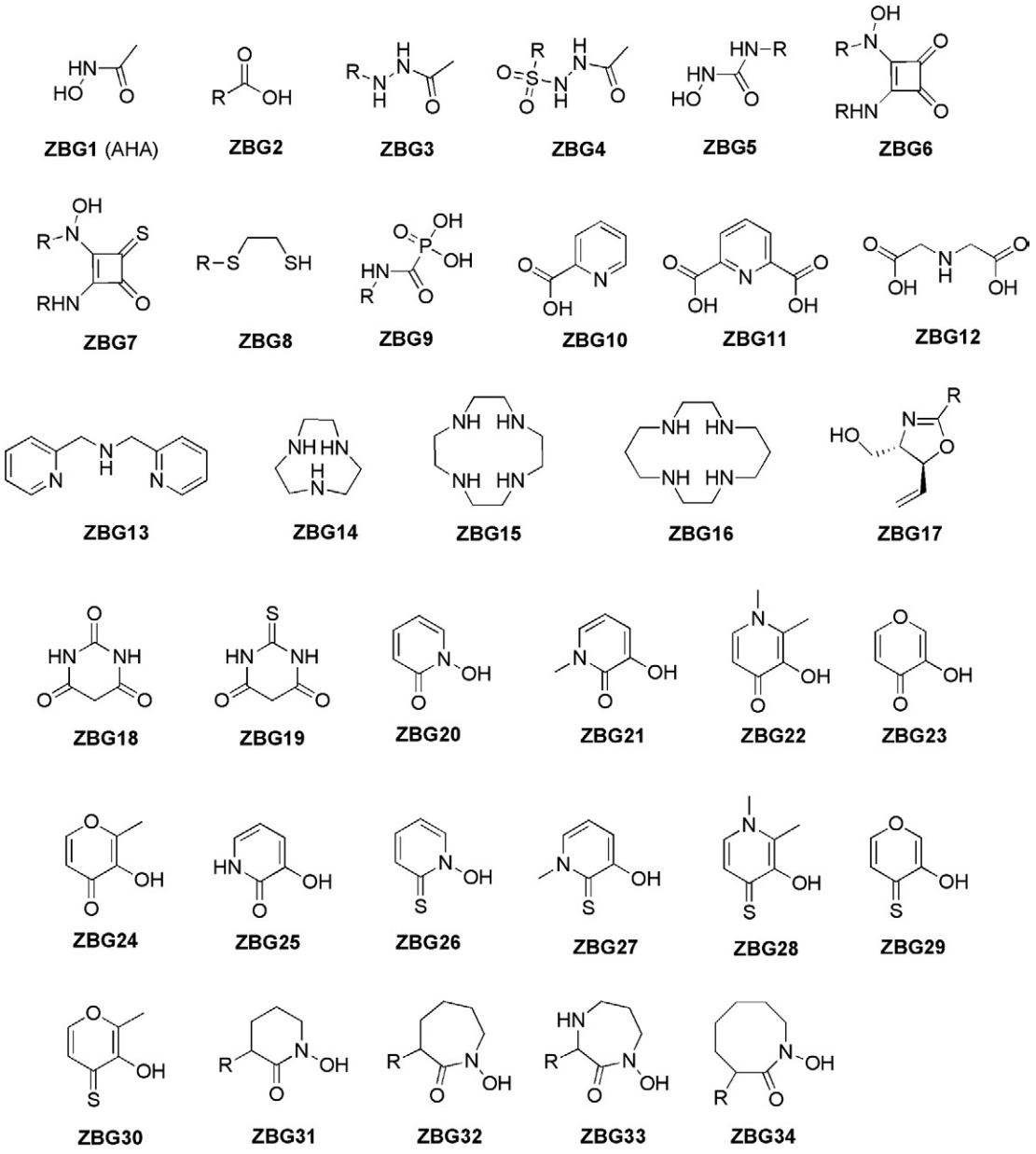

Fig. 4. The structures of ZBGs used in MMPi. The most common ZBG is the hydroxamic acid group, represented here by acetohydroxamic acid (**ZBG 1**, AHA).

3.2. Derivatives of early ZBGs

In 2003, Auge et al. introduced hydrazide (**ZBG3**) and sulfonylhydrazide (**ZBG4**) analogues of the hydroxamate MMPi, Illomastat [79]. The hydrazide ZBG is isosteric to a hydroxamic acid and has the potential for similar bidentate metal chelation (Fig. 5), though the inhibitors obtained were considerably less potent than Illomastat. An important advantage of the hydrazide and sulfonylhydrazide ZBGs is that they can be derivatized to probe both the primed and unprimed side pockets in the active site [80]. Sulfonylhydrazide **9** is a potent inhibitor of MMP-1 (IC_{50} = 30 nM), MMP-2 (IC_{50} = 9.8 nM), and MMP-9 (IC_{50} = 3 nM) [80]. Docking of **9** in MMP-2 and -9 shows that the ZBG can make two hydrogen bonds with the peptide backbone similar to hydroxamic acid inhibitors (Fig. 1). Computational modeling also predicts that the backbone of this inhibitor targets the S2, S1', and S2' pockets.

N-hydroxyurea (**ZBG5**) has also been investigated as an alternative ZBG for MMPi because of its structural similarity to hydroxamic acids and because of the improved oral bioavailability of *N*-hydroxyurea-derived 5-lipoxygenase inhibitors [2,67]. However, Michaelides et al. observed a reduction in potency from the hydroxamic acid MMPi **10** to its *N*-hydroxyurea analogue, **11** [81]. A study by Campestre et al. elucidated this loss in potency by comparison of the structurally related inhibitors **11** and **12** [82]. Due to the ability of *N*-hydroxyureas to adopt a trans N1-CO amide bond conformation, intramolecular hydrogen bonding within the ZBG would preclude effective Zn^{2+} chelation [83]. It was proposed that methylation at N3 of **11** would prevent intramolecular hydrogen bonding within the ZBG and would therefore increase the ability of the inhibitor to chelate Zn^{2+}. Though the *N*-methylated inhibitor **13** was more than twice as potent against MMP-2 as **11**, the compound was still more than 50-fold less potent than **12** against MMP-3. Crystal structures of **12** and **13** with MMP-8 show that the *N*-hydroxyurea inhibitor binds the Zn^{2+} ion only through the terminal hydroxyl group, while the hydroxamate inhibitor chelates the Zn^{2+} ion in a bidentate fashion to form the expected 5-membered ring (Fig. 5). The sp^2 hybridization at N3 may decrease the flexibility of **13** relative to **12**, leading to a binding conformation that did not allow for chelation [82].

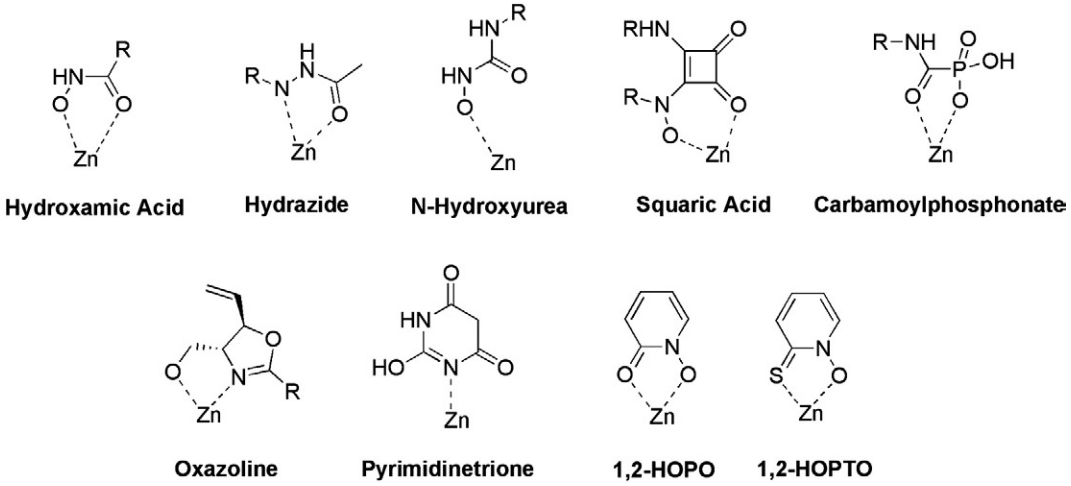

Fig. 5. Binding modes of several representative ZBGs to the Zn^{2+} ion.

Squaric acid-based hydroxamic acid analogues (**ZBG6–7**) were developed into MMPi in an attempt to target MMP-1 [84]. This ZBG forms a 6-membered ring upon metal chelation as opposed to the 5-membered ring of hydroxamic acid (Fig. 5). The thiocarbonyl squaric acid full-length MMPi **14** was found to have an IC_{50} of 15 μM against MMP-1, which was an 18-fold improvement over its carbonyl precursor **15**. The binding mode with squaric acid derivatives may provide a means to uniquely position inhibitors into the substrate-binding pockets that may prove fruitful in the design of selective MMPi in the future. Further development of this ZBG is still necessary to obtain more potent derivatives.

Hurst et al. reported a series of mercaptosulfide (**ZBG8**) inhibitors in 2005 that target MMP-14 [85]. The role of MMP-14 in tumor-cell invasion and metastasis has made it an attractive target for inhibition [86]. Inhibitor **16**, which uses a cyclic mercaptosulfide, was determined to be a competitive inhibitor of the catalytic domain of MMP-14 with a K_i of 24 nM but was found to be more potent for MMP-2 ($K_i = 1.1$ nM) and MMP-9 ($K_i = 0.57$ nM) [85]. A structure–activity relationship study indicated that the pentyl ring of **16** improves the stability of the inhibitor as compared to linear mercaptosulphides, which can be readily oxidized under air and therefore lose their potency [85]. While the desired selectivity was not observed, the utility of the mercaptosulphide inhibitors is that they can be modified to target both the primed and unprimed side pockets of the MMP.

MMPi with phosphorus-based ZBGs have been investigated by several laboratories. Much of this work is focused on the development of α-biphenylsulfonylamino phosphonates, analogues of a known group of MMPi that had been prepared with both carboxylate and hydroxamate ZBGs [87–89]. MMP-8 was used as a model for identifying the characteristic contacts of this inhibitor with residues of the highly conserved MMP active sites. A crystal structure of the *R*-enantiomer of **17** in MMP-8 showed that these ZBGs bind through two phosphonate oxygen atoms in a distorted tetrahedral geometry [87]. It was found that compared to its enantiomer the *R*- stereoisomer of **17** demonstrates better hydrophobic interactions between the isopropyl group of the inhibitor and the S1 pocket residues, shows improved hydrogen bonding with the sulfonamide moiety, and allows for better π stacking of the biphenyl backbone due to deeper S1' insertion. Based on this series, Biasone et al. reported a potent phosphonate inhibitor **18** that exhibits selectivity for MMP-8 over MMP-1, -2, -3, -7, -9, -13, and -14 [88]. Selective MMP-8 inhibitors could be useful in the treatment of acute liver disease and multiple sclerosis [90,91].

Matziari et al. reported a series of phosphinate inhibitors that show high selectivity for MMP-11, a presumed target for tumorigenesis in breast cancer [92]. Compound **19** has a $K_i = 0.11$ μM against MMP-11, which is >30× more potent versus MMP-2, -8, -9, -13, and -14 [92]. Much of the selectivity of the inhibitors is attributed to the P1' interactions with the protein at the entrance to the S1' site. As these inhibitors show specificity for MMP-11 over other deep pocket MMPs, it is implied that the selectivity is not based solely on exploitation of the S1' pocket size, as is common in other inhibitors, but on other protein–inhibitor interactions. In particular, the derivatives that showed the best selectivity were based on phenyl rings that do not insert deeply into the S1' pocket. These results indicate that targeting of MMPi toward the entrance of the S1' pocket rather than deep in the pocket can provide a means to improve selectivity. The use of phosphinic ZBGs may provide improved metabolic stability of MMPi when compared to hydroxamates [92].

Another new phosphorus-based ZBG for MMPi is the carbamoyl phosphonate ZBG (**ZBG9**). Instead of binding through two oxygen atoms of the phosphonate, these ZBGs are proposed, based on calculations, to bind Zn^{2+} through one oxygen of the phosphonate and the oxygen of the carbonyl alpha to the phosphonate in order to form a 5-member chelate ring that resembles the binding of hydroxamic acid (Fig. 5) [93]. The amide bond of the carbamoyl phosphonate may contribute to the improved activity of inhibitors with this ZBG relative to α-ketophosphonate inhibitors because it provides an extra hydrogen bond donor for protein interactions and because the electron donating ability of the amide group allows for stronger Zn^{2+} chelation [94]. The net negative charge on the ZBG prevents cell penetration and restricts these inhibitors to the extracellular space, contributing to their low toxicity [95]. Several inhibitors based on these ZBGs are selective for MMP-2 and were thereby evaluated in both in vitro and in vivo models of tumor invasion and angiogenesis [94]. Specifically, compound **20** inhibits MMP-2 with an IC_{50} of 20 nM yet inhibits MMP-1, -3, -8, and -9 with IC_{50} values of 20 μM or greater [94]. The potency of **20** against MMP-2 is remarkable considering its simplicity and very low molecular weight. This inhibitor provides 40% inhibition at 50 μM in a basement membrane cell invasion assay [94]. When dosed intraperitoneally at 50 mg/kg daily for three weeks in a murine model of melanoma metastasis, **20** shows 55% inhibition of lung metastasis formation [94].

More recently, the biological activity and pharmacokinetics of a carbamoyl phosphonate inhibitor of MMP-2 and -9 (compound **21**) were evaluated more thoroughly [95]. This inhibitor spares MMP-1, -3, -8, -12, and -13 while targeting MMP-2 and -9 with modest potency at 4 μM and 20 μM, respectively. Compound **21** shows a dose-dependent relationship with both inhibition of cell invasion in a

Matrigel assay and in the prevention of tumor colonization in the murine melanoma model. Further, this inhibitor shows efficacy with both oral and intraperitoneal dosing and the minimum inhibitory concentration of **21** is 12 ng/mL [95]. Compound **21** provides 60% reduction in tumor growth and 90% reduction of metastasis at 50 mg/kg in the more aggressive murine model based on orthotopic implantation of human tumor prostate cells in immunodeficient mice [95]. Slow absorption and rapid elimination ($t_{1/2}$ < 20 min for intravenous administration) characterize the pharmacokinetics of this inhibitor [95]. Prolonged absorption accounts for the sustained efficacy of this drug despite a low oral bioavailability of 0.3% [95]. These ZBGs offer the advantages that their inhibitors are water soluble at physiological pH and are not acutely toxic at the concentrations used in the murine models (up to 500 mg/kg for **21**) [95]. The positive pharmacokinetics and selectivity profiles displayed by the carbamoyl phosphonates inhibitors discussed here indicate the potential promise that this ZBG may have to develop clinically relevant selective MMPi. However, obtaining more potent derivatives of these carbamoyl phosphonate MMPi will be an important advancement for this class of compounds.

3.3. Nitrogen-based ZBGs

In 2006, Jacobsen et al. introduced a well-known series of chelators for use as nitrogen-based ZBGs (**ZBG10–16**) [96]. These ZBGs were chosen due to their binding preference for late transition metals. **ZBG10** (picolinic acid) binds Zn^{2+} via bidentate chelation through a carboxylate oxygen and the pyridine nitrogen as determined by the crystal structure of **ZBG10** in the bioinorganic model complex [$(Tp^{Ph,Me})$Zn(**ZBG10**)] ($Tp^{Ph,Me}$ = hydrotris(3,5-phenylmethylpyrazolyl)borate). Compounds **ZBG10** and **ZBG13–15** are all more than 100-fold more potent for MMP-3 over acetohydroxamic acid (AHA, **ZBG1**) [96]. AHA and maltol (**ZBG24**) both inhibit the activity of 5-lipoxygenase, an iron enzyme, at 300 μM, while **ZBG10-16** do not [96]. This supports the hypothesis that use of nitrogen-based ZBGs may improve selectivity towards Zn^{2+}-dependent enzymes. Further synthesis of complete MMPi with these ZBGs is needed to determine if these compounds will be effective in producing selective MMPi.

Oxazolines of the type **ZBG17** have been investigated as another proposed nitrogen-based ZBG [97]. The oxazoline rings are modified at the 4-position with a methylene hydroxyl group to allow for a proposed binding mode via a 5-membered chelate ring between the nitrogen atom of the oxazoline and the oxygen atom of the hydroxyl group (Fig. 5). The relative position of the S1' pocket to the Zn^{2+} ion in MMPs indicates that P1' substituents attached to the 2-position of the oxazoline ring would be favorably directed toward the S1' pocket [97]. The best inhibitor reported based on this ZBG is compound **22**, which is a modest inhibitor of MMP-9 (K_i = 6 μM) that does not inhibit MMP-1, -2, or -12 up to 500 μM [97]. The binding mode of this ZBG has yet to be experimentally determined and more potent inhibitors need to be developed to obtain better structure–activity relationships.

The most extensively studied class of MMPi with nitrogen-based ZBGs are the pyrimidine-2,4,6-trione (and dionethione) inhibitors (Fig. 4, **ZBG18–19**). In 2001, Hoffman-LaRoche published several papers on a series of new MMPi with pyrimidine-2,4,6-trione ZBGs [98–101]. The pyrimidine-2,4,6-trione group is a known feature in many FDA-approved drugs (barbiturate class), and so its metabolic disposition and bioavailability have been well studied [98]. Co-crystal structures of pyrimidine-2,4,6-trione inhibitors in MMP-3 and -8 demonstrate that this ZBG binds to the Zn^{2+} using the N3 nitrogen atom (Fig. 5) [99,101]. The carbonyl oxygen adjacent to the binding nitrogen favors the enol form because it is stabilized by dual hydrogen bonding between the enolate hydrogen and two oxygen atoms of a neighboring glutamic acid residue [99,101]. The O6 and N1 atoms around the ring produce further stabilization through hydrogen bonding with the peptide backbone in the active site [99,101]. Pyrimidine-2,4,6-trione MMPi were first optimized for gelatinase specificity to develop anticancer drugs [98,100]. New MMPi were developed with improved potency for MMP-8, which was used as a model for MMP-2 and -9 due to the structural homology of these targets [98]. Derivitization at the 5-position of this ZBG provides access to target the S1' and S2' subsites [98]. Parallel optimization of the P1' and P2' substituents followed by merging of the optimized inhibitor backbones led to the design of **23**, which inhibits MMP-2, -8, -9, and -14 with IC_{50} values ranging between 10 and 15 nM and MMP-1 and -3 at micromolar concentrations [98]. In 2004, compound **23** was evaluated for anti-invasive, anti-tumorigenic, and anti-angiogenic activity [102]. Compound **23** inhibits chemoinvasion by 85% at concentrations as low as 10 nM and showed anti-cancer efficacy in several in vitro and in vivo models [102].

More recently, pyrimidine-2,4,6-trione MMPi have been optimized to inhibit MMP-13 for the development of anti-osteoarthritis drugs [103–106]. This work started with the development of conformationally restricted spirobarbiturate inhibitors that mimicked the binding geometry of a known MMP-13 hydroxamate inhibitor [103]. Several spirobarbiturate inhibitors with P1' substituents based on diphenylethers have K_i values on the order of 5 nM toward MMP-13 [103]. Extension of the S1' binding diphenylether group with 5-membered heterocycles yielded several inhibitors with >100-fold potency for MMP-13 over MMP-14 [104]. Significant selectivity for MMP-13 over MMP-2, -8, and -12 was obtained with aryl oxazoline derivatives of the diphenylether S1' binding moiety [105]. One such inhibitor, compound **24**, was evaluated in a hamster model to assess its ability to inhibit MMP-13 in the synovial fluid milieu [105]. Compound **24** was found to have an ED_{50} of about 1 mg/kg and inhibited bovine cartilage degradation with an IC_{50} of 40 nM [105]. In addition, no fibroplasias were observed in a rat model of MSS at doses up to 300 mg/kg twice per day [105]. However, spiropyrrolidine barbiturate inhibitors with similar selectivity and in vivo activity produce some rat fibroplasias in this model [106].

3.4. Heterocyclic bidentate ZBGs

In 2004, Puerta et al. introduced a series of heterocyclic bidentate chelators **ZBG20–30** for development as alternative ZBGs in MMPi [72]. These ZBGs were chosen because they have some features in common with hydroxamic acids (5-member chelates, monoanionic) but with potentially better biostability and tighter Zn^{2+} binding due to ligand rigidity and, in some cases, the incorporation of sulfur donor atoms. The binding modes of most of these compounds were verified by characterization of an active site model system [$(Tp^{Ph,Me})$Zn(ZBG)] [72,107,108]. In vitro assays showed these ZBGs all inhibited MMP-1, -2, and -3 with greater potency than AHA: up to 15-fold improvement for O,O chelators and up to 700-fold for O,S chelators [72,73]. Cell viability assays show that the O,O chelators have low toxicity at concentrations as high as 1 mM, while the O,S chelators start to reduce cell viability at concentrations above 100 μM [73]. In a cell invasion assay, **ZBG20** is the only O,O chelator that was able to inhibit cell invasion at 1 mM, but several O,S chelators, **ZBG26**, **ZBG27**, **ZBG28**, and **ZBG30**, are able to inhibit cell invasion at 100 μM [73].

Several of these ZBGs have been developed into complete MMPi with good potency [75–78]. Relative to the ZBGs, the full-length inhibitors are significantly more potent and show some selectivity between MMPs. Compound **25** is a full-length inhibitor based on **ZBG24** with an amide linkage to a terphenyl backbone that is >2500-fold more potent for MMP-3 (IC_{50} = 19 nM) over MMP-1 and -2 [76]. Compound **26** is a nanomolar inhibitor of MMP-12 that is also potent against MMP-2, -3, and -8 but is significantly less effective against MMP-1, -7, -9, and -13 [75]. Inhibitor **26** was tested in an ex vivo rat heart model of ischemia and reperfusion. Hearts treated with 5 μM **26** were found to recover >80% of their original contractile function versus 50% for untreated hearts [75].

In 2008, Zhang et al. explored several alternative ZBGs inspired by **ZBG20** that included expanded non-planar rings (**ZBG31**–**34**) [78]. These ZBGs are 6-, 7-, and 8-membered heterocyclic chelators, including 1-hydroxy-2-piperidinone, 1-hydroxyazepan-2-one, 1-hydroxyazocan-2-one, and 1-hydroxy-1,4-diazepan-2-one. Because these heterocycles are not unsaturated (nor aromatic) and hence not planar, bond rotation is less restricted and this can result in out-of-plane twisting of the chelating oxygen atoms. This decreases the binding affinity of these ZBGs as compared to **ZBG20**, and it was found that, given the same backbone, **ZBG20** provided the most potent inhibitor. Following these findings, inhibitor **27**, which uses **ZBG20**, was developed and shown to have IC_{50} values ranging from 2.4 to 5.0 nM against MMP-2, -9, and -13 and was selective over MMP-1 ($IC_{50}>1$ μM) and moderately selective over MMP-3 ($IC_{50}=56$ nM) [77]. Compound **27** exhibits an elimination half-life of 47 h in rats dosed at 2 mg/kg intravenously and also demonstrates a reduction in brain edema following ischemia–reperfusion in a mouse transient mid-cerebral artery occlusion (tMCAO) model [77].

In a systematic study, MMPi **26** and **28–31**, each containing a different ZBG connected to the same biphenyl backbone, were examined against a series of MMPs [75]. These five MMPi have different selectivity profiles, supporting the idea that the ZBG can influence specificity. For example, the pyrone-based inhibitor **28** has an IC_{50} value of 77 nM against MMP-3, while the IC_{50} value of the hydroxypyridinone derivative **29** is 41.7 μM [75]. Similarly, compound **30** inhibits MMP-3, -8, and -12 with IC_{50} values ranging from 22 to 240 nM, while the IC_{50} values of **31** against all of these MMPs are above 5 μM [75]. Computer modeling of compounds **30** and **31** in the active site of MMP-3 suggests that unfavorable steric interactions between the ZBG in compound **31** and the protein may account for the differences seen in the activity of these two MMPi [75]. This systematic study, using a single common backbone with different ZBGs, provides compelling evidence that even tight-binding ZBGs can play a role in tuning MMPi selectivity.

Just as changes in the ZBG can generate differences in selectivity, changes in the connectivity and point of attachment of the ZBG to the backbone can also result in dramatic changes in potency and selectivity. For example, MMPi **30** has an IC_{50} value of 240 nM against MMP-3 [75,76]; however, the direct structural isomer of this inhibitor, MMPi **32**, shows only weak inhibition (~30%) at concentrations as high as 100 μM [109]. This comparison shows that two MMPi with the same chemical formula, ZBG, and backbone can have vastly different activities based solely on the relative positioning of the backbone on the ZBG. Furthermore, the analog of **32** that utilizes a sulfur donor atom (**33**) was also found to have very different MMP inhibition profiles [109]. In a related comparison using **ZBG20**, inhibitor **26** was found to be a semi-selective inhibitor with nanomolar activity against MMP-3, -8, and -12 [75]. However, linking of a backbone to the 3-position in compound **27** (Fig. 7), rather than the 5-position (as in **26**), of **ZBG20** led to a series of potent inhibitors against MMP-2, -9, and -13 [77,78]. In both of the aforementioned examples, inhibitors have identical or similar backbones and identical ZBGs but show dramatically different MMP selectivity and potency based on the point of attachment of the ZBG. Because the primary difference is the position of the backbone on the heterocyclic ZBG, it is likely that a change of the backbone orientation in the MMP active site is responsible for the change in inhibitory behavior. This suggests another means to exploit novel ZBGs for improved selectivity, whereby the ZBG is used to preferentially position inhibitor backbones toward different subsites to obtain optimal selectivity. Such an approach can not be employed using traditional hydroxamic acid or carboxylic acid ZBGs. A better understanding of the role of the ZBG in generating selectivity may provide another route to obtaining selective inhibitors.

4. 'Or not to bind zinc': non-zinc-binding MMPi

Over the last several years, numerous MMPi have been reported that do not possess a ZBG and hence do not bind the catalytic Zn^{2+} ion (Table 3, compounds **34**–**39**) [41,110–116]. The rationale for this strategy is that minimizing or eliminating the interaction with the catalytic Zn^{2+} ion best achieves MMP selectivity, as the metal site is the most conserved feature across all MMPs. Nearly all of these inhibitors show impressive MMP-13 selectivity and bind deep within the S1' pocket to induce a specific protein conformation. Several inhibitors from this class show promise in the treatment of osteoarthritis in animal models [41,110].

Certain structural features are thematic across this class of inhibitors. All tend to be fairly long molecules with linked ring structures that are aromatic or otherwise planar. While the inhibitors are generally hydrophobic, carbonyl oxygen atoms and N–H groups offer opportunities for hydrogen bonding interactions with the S1' pocket. Some non-zinc-binding MMPi have hydrophilic ends that have been shown, based on crystallographic data and molecular docking studies, to extrude into solvent-exposed areas from the active site [110,111,113].

Most non-zinc-binding inhibitors have been characterized by crystal structures with MMP-8, -12, or -13 [41,111–113,116]. These structures confirm that these MMPi have no significant interactions with the Zn^{2+} ion, with the closest ligand–zinc distances on the order of ~5 Å [111,112]. It is of note that while the inhibitors have been crystallized with a number of MMPs, all of the compounds are generally selective for MMP-13 (see Table 3). While each of the crystallized MMPi is structurally distinct, many of their protein binding interactions seem to be conserved. Backbone hydrogen bonds, hydrophobic aromatic interactions, and protein flexibility are the key features of these inhibitor–protein complexes. The interactions of a representative inhibitor **34** with MMP-13 are highlighted in Fig. 6 [41]. The phenyl group of the benzyl ester of **34** is aligned almost in parallel with the plane of His^{201}. The carbonyl oxygen of the ester is twisted to allow for hydrogen bonding with the amide backbone of Thr^{224}. The other two carbonyl oxygen atoms form hydrogen bonds to the amide backbones of Thr^{226} and Met^{232}. Both faces of the terminal benzyl group are involved in aromatic edge–face interactions with the side chains of Tyr^{225} and Phe^{231}. Gly^{227} is rotated to a main chain conformation, which opens the S1' pocket to accommodate the inhibitor.

Crystallization studies of these non-zinc-binding MMPi often involve co-crystallization with AHA (**ZBG1**) to prevent autolysis. Morales et al. showed that AHA is not displaced by the non-zinc-binding inhibitors when crystallized in MMP-12 (**35** and **36**) [111]. A similar observation was made by Johnson et al. with inhibitors **34** and **37** in MMP-13 (Fig. 6) [41]. It is important to consider that the presence of AHA in the crystallization conditions may predispose the positioning of the inhibitor to a non-zinc-binding orientation that is different than would be observed in the absence of AHA. However, other crystal structures of non-zinc-binding MMPi do show similar hydrogen bonding interactions with the inhibitor and protein backbone; one example is compound **38** co-crystallized with MMP-12 [112].

The kinetics of several non-zinc-binding MMPi show a non-competitive mechanism of inhibition. Gooljarsingh et al. recently described the kinetics of a pyrimidine dicarboxamide inhibitor **39** and compared it to the kinetics of AHA (**ZBG1**) and a hydroxamate MMPi [115]. Through dual inhibition studies, it was found that AHA and the hydroxamate-based MMPi act as competitive inhibitors, while the non-zinc-binding **39** was non-competitive. Further, when the hydroxamates were tested in concert with **39**, it was found that AHA led to synergistic potency with **39**, while the bulky hydroxamate was antagonistic. Modeling studies showed overlap between the binding space of the large hydroxamate and **39** but showed independent

Table 3
Structures and IC_{50} values (μM) of non-zinc-binding MMPi.

ID	Structure	IC_{50} value (μM)									Ref.
		MMP-1	MMP-2	MMP-3	MMP-7	MMP-8	MMP-9	MMP-12	MMP-13	MMP-14	
34	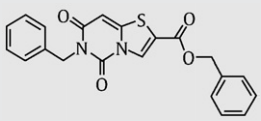	>100	>100	>100	>100	>100	>100	>100	0.03	>100	[41]
35	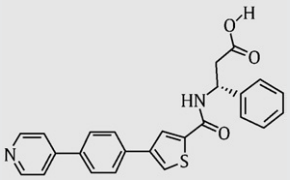	>100	0.39	1.7		0.98	1.4	0.014	0.27		[111]
36	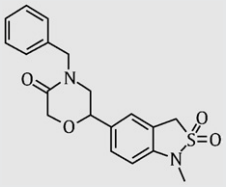	>100	6.6	>100		5.1	>100	24	4.9		[111]
37	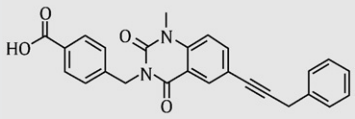	>30	>30	>30	>30	>100	>100	>100	0.00067	>30	[41]
38	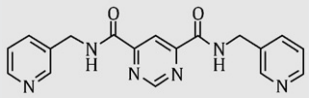	NI	NI	NI	NI	NI	NI	NI	6.6	NI	[112]
39	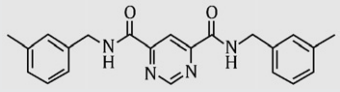								0.072		[112]

NI = no inhibition at concentrations up to 100 μM.

binding sites for **39** and AHA, which is consistent with the experimental findings. Johnson et al. also found that a non-competitive mechanism of inhibition best described the kinetics of **34** [41]. The crystal structure of this inhibitor with MMP-13 shows that it binds deep in the S1' site where there is no overlap with the natural substrate-binding space [41].

As stated earlier, most of the non-zinc-binding MMPi show remarkable selectivity for MMP-13 [41,110–112]. Among the best is **37**, which inhibits MMP-13 with an IC_{50} value of 0.67 nM but does not appreciably inhibit MMP-1, -2, -3, -7, -8, -9, -12, -13, -14, or -17 up to 100 μM. The source of the selectivity for **37** has been attributed to specific S1' binding interactions observed in structures of similar compounds (Fig. 6) and to the general differences in the shape and size of S1' pockets across the various MMPs. Selectivity of **37** over MMP-1, -2, -7, -8, and -9 is due to the shorter S1' specificity pockets, which may not be able to accommodate the especially long P1' substituents of **37**. Additionally, as discussed earlier, the MMP-13 S1' pocket displays substantial flexibility. While many crystal structures with zinc-binding inhibitors show disorder in the S1' region, it is notable that in several of the structures with non-zinc-binding inhibitors, the S1' pockets are crystallographically well-defined [41,112]. Binding of these inhibitors may rigidify the enzyme active site into a specific conformation that is less productive for substrate binding. The flexibility of MMP-13, relative to other MMPs, may allow for this favorable conformation where it is not accessible in other MMPs. Specifically, certain glycine residues (Gly^{227} and Gly^{248} with **34** and **38** inhibitors, respectively) in MMP-13 rotate relative to the main chain conformation in the inhibitor-bound protein structure [41,112]. With each of these rotations, the S1' pocket opens to an exosite, which extends the pocket length and allows the protein to accommodate the long inhibitors. Inhibitor binding prevents the glycine residue from rotating back to a side chain conformation and thereby rigidifies the pocket structure. This would explain the conformational order seen in the S1' site of these inhibitor complex structures of MMP-13. It may also account for the high affinity of these inhibitors for MMP-13. Because these glycine residues are not conserved in other MMPs and

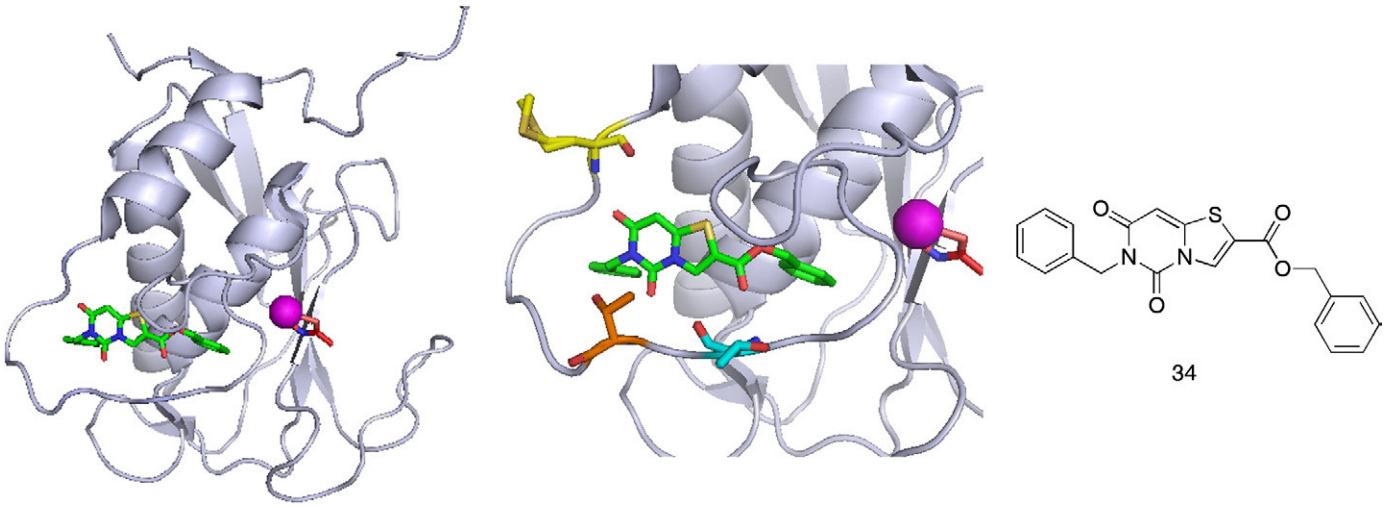

Fig. 6. Left. Ribbon structure of MMP-13 (grey) co-crystallized with the non-zinc-binding inhibitor, **34** (highlighted in green), and acetohydroxamic acid (highlighted in red) (PDB code 2OW9) [41]. Right. Magnified view of **34** in S1' specificity loop highlighting the hydrogen-bonded residues Thr^{224} (cyan), Thr^{226} (orange), and Met^{232} (yellow). The catalytic Zn^{2+} ion is represented as a purple sphere in both views.

the rotated main chain conformation is energetically unfavorable for other residues, decreased affinity for other MMPs would be expected. Similar induced conformations have been observed in the crystal structures of MMP-8 with non-zinc-binding inhibitors [116].

As most of these non-zinc-binding MMPi are potent and selective, derivatives have aimed to improve their drug-like properties [110,113]. The hydrophobicity of these inhibitors is critical in maintaining productive protein–inhibitor interactions that result in high potency; however, it also results in poor water solubility. In order to improve the solubility with minimal effect on potency, derivatives have been explored to specifically modify the solvent-exposed portions of the molecule while maintaining the hydrophobic core structures. Dublanchet et al. found that carboxylic acids positioned toward solvent-exposed parts of the molecule help to significantly solubilize MMPi that are otherwise poorly soluble [113].

Preclinical studies with **37** in models of osteoarthritis have shown encouraging results [41]. Compound **37** was found to have an efficacy at doses as low as 0.1 mg/kg in an MMP-13-induced rat model of cartilage knee joint damage. This model was used to show that **37** had in vivo activity in a relevant disease system and to establish the dosing efficacy to determine the viable modes of drug administration. Oral dosing twice daily at 30 mg/kg of **37** resulted in a 68% reduction in the cartilage legion area of tibial plateaus in rats with surgically induced cartilage knee damage. The rat joints were subsequently examined for evidence of fibroplasias and expanded inner synovial lining, which are indicative of MSS. The fibroplasias were absent in all vehicle and rats dosed with compound **37** but present in all rats dosed with broad-spectrum MMPi. Inhibitors of this kind, with such a high degree of selectivity, may become an important solution to the toxic side effects associated with broad-spectrum MMP inhibition. However, this strategy is limited by the design challenges posed in obtaining such highly selective MMPi. Additionally, it is often unknown how relevant certain MMPs are to disease processes; identification of diseases that respond significantly to inhibition of only one MMP may be challenging.

These non-zinc-binding inhibitors are remarkable primarily because of their high selectivity. It is clear that a major reason for the selectivity of **34** and **38** is their ability to induce a unique conformation in the S1' specificity loop of MMP-13 that is not accessible in other MMPs [41,112]. It is not yet clear if the observed selectivity of these inhibitors actually relies on the fact that there is no ZBG present. A comparison between one of these inhibitors and an inhibitor that can both induce a conformational change in the MMP-13 S1' pocket and chelate the active site Zn^{2+} ion would provide significant insight on this topic.

5. Mechanism-based MMPi

In 2000, Mobashery and coworkers introduced SB-3CT (Table 4, **40**) as the first mechanism-based inhibitor of MMPs (Fig. 7) [117]. This inhibitor binds in the active site and forms a covalent bond with the protein upon activation by Zn^{2+} coordination. The formation of the covalent bond impedes inhibitor dissociation relative to traditional, chelating, competitive inhibitors. This ensures that the rate of catalytic turnover is reduced, and therefore, less inhibitor is needed to saturate the enzyme active sites. Compound **40** is a selective inhibitor of MMP-2 and -9 and shows promise in pre-clinical studies as an inhibitor of bone metastasis in prostate cancer and in the prevention of damage caused by cerebral ischemia.

The structure of **40** is relatively simple, which is reflected by its low molecular weight [117]. The backbone of **40** is a diphenylether, a well-known S1' binding moiety that is present in many MMPi [77,78,103,118–124]. The inhibitor coordinates the Zn^{2+} via the sulfur of its thiirane ring. No crystallographic data of inhibitor binding in the protein active site is available; however, monodentate coordination to generate a tetrahedral Zn^{2+} center was confirmed by X-ray absorption spectroscopy [125]. The backbone and thiirane ring are connected by a sulfone group and a methylene linker. The oxygen atoms of the sulfone are proposed to form hydrogen bonds with amide hydrogen atoms from the backbone of two active site residues: Leu^{191} and Ala^{192} (numbering for MMP-2) [117]. This hydrogen bonding has been seen in other sulfone inhibitors [87,89]. Inhibitors with two or three methylene groups between the sulfone and the thiirane ring are inactive [117]. These inhibitors do not properly position the thiirane ring within the Zn^{2+} coordination sphere.

The mechanism of inhibition of **40** is similar to that of a “suicide substrate” in which a functional group is activated, leading to covalent modification of the enzyme active site [117,126]. It is proposed that the thiirane group of **40** activates upon Zn^{2+} coordination (Fig. 7), which results in ring opening via a nucleophilic attack from an active site glutamic acid residue (Glu^{404}) forming a covalent ester bond between the carbon from the thiirane ring and Glu^{404} [117]. This bond tethers the inhibitor in the active site, thereby resulting in low inhibitor dissociation. Upon inhibitor binding, the Zn–S bond with **40** is at a distance of 2.22 Å, comparable to the Zn–S bond with cysteine (2.24 Å) of the pro-enzyme [125,127]. This indicates that a thiolate group strongly coordinates Zn^{2+} in the inhibited complex and supports the proposed mechanism of inhibitor activation [125].

Table 4
Structures and K_i (μM) values of mechanism-based MMPi.

ID	Structure	K_i value (μM)						Ref.
		MMP-1	MMP-2	MMP-3	MMP-7	MMP-9	MMP-14	
40	SB-3CT 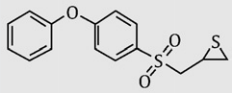	73	0.028	4	67	0.400	0.110	[137]
41	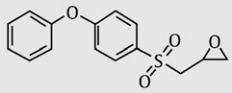	NI	25	NI	NI	186		[117]
42	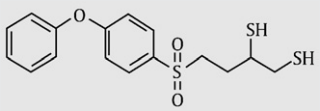	NI	0.046	10	NI	0.100	0.21	[131]
43	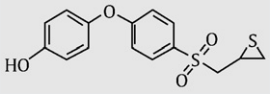	128	0.006	2.2	31	0.16	0.09	[137]
44	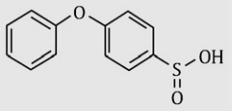							[137]
45	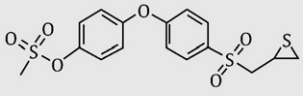	140	0.023	0.600	18.2	0.005	0.145	[139]

NI = no inhibition at concentrations up to 60 or 130–330 μM (see refs. [117,131] for details).

Compound **40** exhibits slow-binding kinetics with MMP-2, -3, and -9, with a time scale for the establishment of equilibrium between the enzyme and inhibitor and the enzyme–inhibitor complex on the order of seconds to minutes [126]. Slow-binding inhibition is characterized by slow dissociation rates (k_{off}), though the binding rate (k_{on}) can be slow or fast [126]. The rate of dissociation of **40** from MMP-2 and -9 is on the order of 10^{-4} s^{-1}. Progress curves, which display enzyme activity over time of MMP-2, -9, and -3 with **40**, are non-linear [117]. The curves show that the initial enzyme rate is not maintained and is instead reduced to a new "steady-state rate" of MMP activity. This indicates a slow-binding mechanism of inhibition and is characteristic of an enzyme with an inhibitor that resists dissociation. The binding of **40** in MMPs is nearly irreversible. Following 95% inhibition, MMP-2 regains 50% activity only after 3 days with dialysis, even though the recovery time calculated based on the k_{off} value is 6 min (without dialysis) [117]. The fact that there is any recovery indicates the inhibitor exhibits some reversibility. This can be attributed to the lability (due to slow hydrolysis) of the ester bond that is formed upon inhibitor activation and binding [117]. The small degree of reversibility of **40** is what distinguishes it from a true suicide inhibitor, which operates strictly by an irreversible mechanism [117,126].

The selectivity of **40** is based on the differences in binding kinetics for various MMPs. As demonstrated by the non-linear progress curves, inhibition increases over time, as slow-binding inhibitors do not dissociate readily from the active site. **40** has nanomolar K_i values for MMP-2 (28 nM), MMP-9 (400 nM), and MMP-14 (110 nM) [128,129]. However, **40** inhibits MMP-2 and -9 via a slow-binding mechanism while inhibition of MMP-14 occurs through competitive inhibition. This difference in kinetics has been proposed as the rationale for the observed selectivity that **40** shows for MMP-2 and -9 over MMP-14 [129].

Several structural variations of the thiirane ring have been explored in an attempt to better understand the activity of **40**. The effect of the stereochemistry of the thiirane ring was examined through synthesis and evaluation of the enantiomers of **40**. Surprisingly, both *R*- and *S*- stereoisomers are active MMPi [128]. However, derivatives containing an epoxide ring such as **41** instead of thiirane are inactive against all MMPs tested even at high micromolar concentrations [117,130]. Several inhibitors were made in which the thiirane ring of **40** was changed to a dithiol, such as compound **42** [131]. In contrast to **40**, it was found that the carbon length between the sulfone and the thiols could be varied without significantly reducing the activity of the inhibitors.

In preclinical studies, **40** has yielded anti-cancer results for both a T-cell lymphoma model and a prostate cancer model [132–134]. In vitro Matrigel tests showed that 1 μM of **40** reduces the invasion ability of BMEC-1 tumor cells by 30% as compared to the vehicle control [133]. Compound **40** was tested in a mouse model of T-cell lymphoma with a dosing range of 5–50 mg/kg/d and was found to promote a dose-dependent reduction in the number of liver

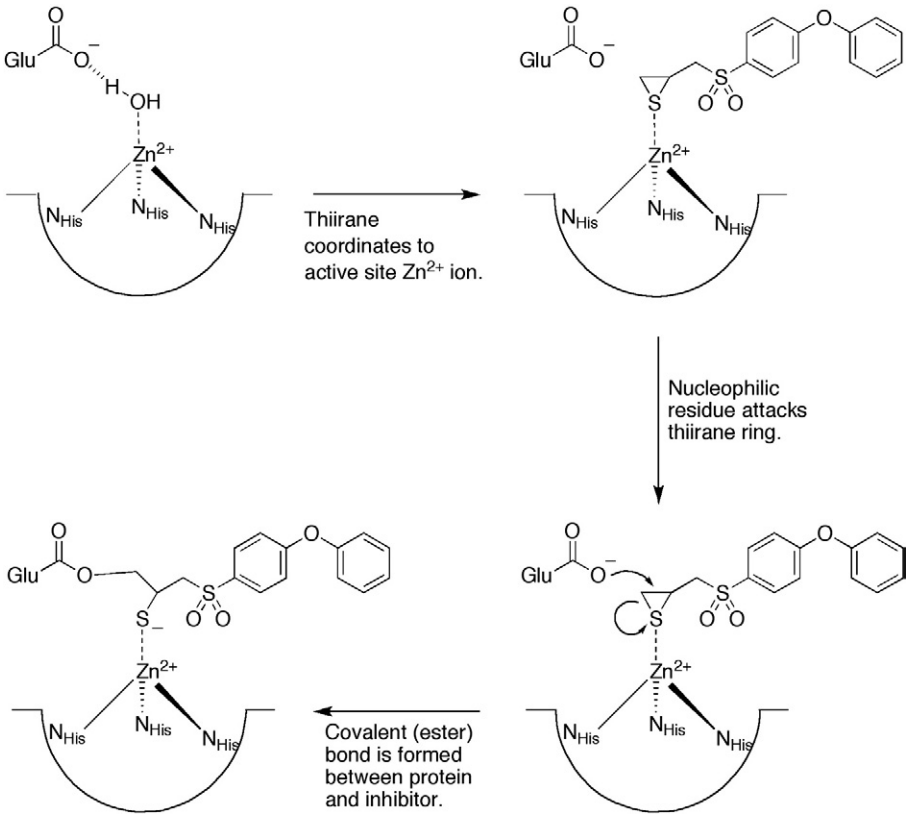

Fig. 7. Scheme for the activity of mechanism-based MMPi (SB-3CT, **40**).

metastases [132]. At 50 mg/kg/d, **40** inhibits liver metastases by 73% and significantly reduces the colony size of the metastases, while the broad-spectrum inhibitor Batimastat (**1**) led to increased metastasis in the same tumor model [132,135]. Additionally, in vitro tests show that the inhibitor does not affect cell growth or viability up to 12.5 μM [132]. Promising results with **40** in a bone metastasis model of prostate cancer show reduced tumor growth and angiogenesis [133].

The use of **40** in a murine stroke model provides significant neuronal protection [136]. Infarct volume is decreased to 30% of the control in mice treated with **40** either prior to or 2 h following ischemia induced by right middle cerebral artery occlusion. Administration of **40** is protective up to 6 h after the ischemic event in mice. Neurological behavioral scores evaluated 24 h after reperfusion show that **40**-treated mice exhibit significant improvements as compared to the control mice, correlating to the observed infarct volumes.

Though it has significant in vivo activity, **40** undergoes rapid metabolism in mice [137]. This leads to low systemic exposure and suggests that a metabolite of the parent compound may be responsible for the in vivo activity. Eight metabolites of **40** were identified in the plasma and urine of mice following intraperitoneal administration of the inhibitor, two of which are primary metabolites (Table 4, **43** and **44**) [137,138]. Metabolite **43** is a more potent inhibitor of MMP-2, -3, -7, -9, and -14 than **40**. Additionally, it demonstrates slow-binding kinetics with MMP-2, -9, and -14 [137]. Analysis of the metabolites led to the design of derivatives that have better in vivo stability and provide longer systemic exposure [139]. Computational modeling and analysis of major metabolites of **40** indicates that the terminal aromatic ring would be best modified at the 4-position with a sulfonate moiety to block one of the major metabolic pathways of the original inhibitor [139]. Inhibitor **45** is a slow-binding inhibitor of MMP-2 and -9 but a competitive inhibitor of other MMPs. Interestingly, the inhibitor is more potent for MMP-9 than MMP-2 ($K_i = 5$ nM and 23 nM, respectively). The metabolites of **45** are 75% more stable than those of **40**, resulting in significantly higher systemic exposure.

SB-3CT and its successors show great clinical promise. The use of mechanism-based, slow-binding inhibitors may provide a new approach to gain selectivity in MMPi design. Other types of covalent modification in the active site may lead to new patterns of selectivity. It will be interesting to see if this class of inhibitors can be expanded to explore selectivity toward other MMPs.

6. Outlook

Improvements in the design of selective MMPi have been realized over the last several years. In addition, studies suggest that semi-selective MMPi may fare better clinically than their broad-spectrum predecessors; however, this may require the development of inhibitors with very narrow windows of activity. Therefore, it is necessary that creative new approaches to address the challenges of obtaining a high degree of MMP selectivity be uncovered. This review has focused on three such approaches, namely, MMPi based on alternative ZBGs, non-zinc-binding MMPi, and mechanism-based MMPi. Each of these approaches has potential as a distinct means to discover MMPi with improved selectivity and biological properties.

A wide array of novel ZBGs has been introduced in recent years that has greatly expanded the number of chemical 'platforms' from which potent MMPi can be developed. Like hydroxamic acids, inhibitors based on these new ZBGs exhibit kinetics of competitive inhibition. In some cases, novel ZBGs allow for incorporation of multiple backbones targeting both sides of the active site (so-called double-handed inhibitors), which has great potential for attaining MMPi selectivity across a number of MMPs. While selective MMPi have been developed with new ZBGs, there continue to be valid concerns that the use of strong metal chelators may preclude the development of highly selective MMPi due to the highly conserved nature of the Zn^{2+} active

site across all MMPs. Many challenges remain for these MMPi, including demonstrations of significant enhancements in MMP selectivity as well as selectivity over other metalloenzymes. In addition, more studies on the bioavailability and pharmacokinetics of these MMPi are required to determine if improvements in these properties are indeed conferred by these compounds.

In contrast to the use of novel ZBGs, substantial success has been achieved with the fundamentally opposite approach, that is, MMPi that do not possess a ZBG at all. This method has proven to be an excellent route for development of selective MMPi for deep pocket MMPs, specifically MMP-13. Unlike inhibitors that employ Zn^{2+} chelation, these compounds display a non-competitive mechanism of inhibition. An advantage of non-zinc-binding MMPi is a potential reduction in non-specific, off-target metalloenzyme inhibition. To date, the use of non-zinc-binding MMPi relies on the intrinsic flexibility of the S1' specificity loop, which is why this method has proven most useful for the development of MMP-13 selective inhibitors. The major challenge for these MMPi is whether selective inhibition of other MMPs will be forthcoming.

Another innovative approach to improved MMPi are mechanism-based inhibitors, in which the inhibitor binds in the active site and is activated to form a covalent adduct with the protein. These MMPi exhibit slow-binding inhibition characterized by slow dissociation rates and a reduced steady-state rate of MMP activity. This strategy relies on the nucleophilic attack from an active site glutamic acid residue that is conserved in all MMPs. The conserved nature of the glutamic acid suggests that this approach should be widely applicable across many different MMPs. It is important to note that metalloproteinases other than MMPs also have active site residues that may be susceptible to these inhibitors [43,140]. Demonstration of new MMP selectivity in these mechanism-based MMPi and additional information on their in vivo activity remain important milestones for this class of compounds.

As this review highlights some of the recent approaches in MMP inhibition, it is evident that much work remains to develop these compounds into clinically successful MMPi. Each new approach has its unique advantages as well as its specific challenges that remain to be overcome. It is imperative that future studies on MMPi should include assessments against a wide battery of MMPs and other metalloproteinases in order to verify target specificity. With so many inventive approaches in the development of next-generation MMPi, it is clear that the opportunities for discovering clinically relevant compounds remain strong.

Acknowledgements

We thank Arpita Agrawal and Dr. Matthieu Rouffet for assistance with an earlier draft of this manuscript. The authors' research on MMP inhibitors is supported by the University of California, San Diego, the National Institutes of Health (R01 HL00049-01), and the American Heart Association (0970028N). J.L.M.J. is supported by a National Institutes of Health Training Grant (5 T32 HL007444-27).

References

[1] J. Hu, P.E. Van den Steen, Q.-X.A. Sang, G. Opdenakker, Matrix metalloproteinase inhibitors as therapy for inflammatory and vascular diseases, Nat. Rev., Drug Discov. 6 (2007) 480–498.
[2] M. Whittaker, C.D. Floyd, P. Brown, A.J.H. Gearing, Design and therapeutic application of matrix metalloproteinase inhibitors, Chem. Rev. 99 (1999) 2735–2776.
[3] E. Nuti, T. Tuccinardi, A. Rossello, Matrix metalloproteinase inhibitors: new challenges in the era of post broad-spectrum inhibitors, Curr. Pharm. Des. 13 (2007) 2087–2100.
[4] H. Nagase, J.F. Woessner Jr., Matrix metalloproteinases, J. Biol. Chem. 274 (1999) 21491–21494.
[5] S.D. Shapiro, Matrix metalloproteinase degradation of extracellular matrix: biological consequences, Curr. Opin. Cell Biol. 10 (1998) 602–608.
[6] H. Nagase, R. Visse, G. Murphy, Structure and function of matrix metalloproteinases and TIMPs, Cardiovasc. Res. 69 (2006) 562–573.
[7] D.E. Gomez, D.F. Alonso, H. Yoshiji, U.P. Thorgeirsson, Tissue inhibitors of metalloproteinases: structure, regulation and biological functions, Eur. J. Cell Biol. 74 (1997) 111–122.
[8] K. Maskos, Crystal structures of MMPs in complex with physiological and pharmacological inhibitors, Biochimie 87 (2005) 249–263.
[9] L.M. Coussens, B. Fingleton, L.M. Matrisian, Matrix metalloproteinase inhibitors and cancer: trials and tribulations, Science 295 (2002) 2387–2392.
[10] A.F. Chambers, L.M. Matrisian, Changing views of the role of matrix metalloproteinases in metastasis, J. Natl. Cancer Inst. 89 (1997) 1260–1270.
[11] C.M. Overall, O. Kleifeld, Validating matrix metalloproteinases as drug targets and anti-targets for cancer therapy, Nat. Rev., Cancer 6 (2006) 227–239.
[12] M. Egeblad, Z. Werb, New functions for the matrix metalloproteinases in cancer progression, Nat. Rev., Cancer 2 (2002) 161–174.
[13] A.R. Nelson, B. Fingleton, M.L. Rothenberg, L.M. Matrisian, Matrix metalloproteinases: biologic activity and clinical implications, J. Clin. Oncol. 18 (2000) 1135–1149.
[14] C. Lopez-Otin, L.M. Matrisian, Emerging roles of proteases in tumour suppression, Nat. Rev., Cancer 7 (2007) 800–808.
[15] G.A. Rosenberg, E.Y. Estrada, J.E. Dencoff, C.Y. Hsu, Matrix metalloproteinases and TIMPs are associated with blood–brain barrier opening after reperfusion in rat brain, Stroke 29 (1998) 2189–2195.
[16] P.G. Mitchell, H.A. Magna, L.M. Reeves, L.L. Lopresti-Morrow, S.A. Yocum, P.J. Rosner, K.F. Geoghegan, J.E. Hambor, Cloning, expression, and type II collagenolytic activity of matrix metalloproteinase-13 from human osteoarthritic cartilage, J. Clin. Invest. 97 (1996) 761–768.
[17] A. Churg, R.D. Wang, H. Tai, X. Wang, C. Xie, J. Dai, S.D. Shapiro, J.L. Wright, Macrophage metalloelastase mediates acute cigarette smoke-induced inflammation via tumor necrosis factor-alpha release, Am. J. Respir. Crit. Care Med. 167 (2003) 1083–1089.
[18] R.D. Hautamaki, D.K. Kobayashi, R.M. Senior, S.D. Shapiro, Requirement for macrophage elastase for cigarette smoke-induced emphysema in mice, Science 277 (1997) 2002–2004.
[19] B.G. Rao, Recent developments in the design of specific matrix metalloproteinase inhibitors aided by structural and computational studies, Curr. Pharm. Des. 11 (2005) 295–322.
[20] D. Georgiadis, A. Yiotakis, Specific targeting of metzincin family members with small-molecule inhibitors: progress toward a multifarious challenge, Bioorganic Med. Chem. 16 (2008) 8781–8794.
[21] S. Brown, S.O. Meroueh, R. Fridman, S. Mobashery, Quest for selectivity in inhibition of matrix metalloproteinases, Curr. Top. Med. Chem. 4 (2004) 1227–1238.
[22] C.M. Overall, O. Kleifeld, Towards third generation matrix metalloproteinase inhibitors for cancer therapy, Br. J. Cancer 94 (2006) 941–946.
[23] D.R. Shalinsky, J. Brekken, H. Zou, C.D. McDermott, P. Forsyth, D. Edwards, S. Margosiak, S. Bender, G. Truitt, A. Wood, N.M. Varki, K. Appelt, Broad antitumor and antiangiogenic activities of AG3340, a potent and selective MMP inhibitor undergoing advanced oncology clinical trials, Ann. N.Y. Acad. Sci. 878 (1999) 236–270.
[24] D.E. Becker, Drug therapy in dental practice: general principles. Part 2. Pharmacodynamic considerations, Anesth. Prog. 54 (2007) 19–24.
[25] B. Fingleton, MMPs as therapeutic targets—still a viable option? Semin. Cell Dev. Biol. 19 (2008) 61–68.
[26] P. Vihinen, R. Ala-aho, V.-M. Kahari, Matrix metalloproteinases as therapeutic targets in cancer, Curr. Cancer Drug Targets 5 (2005) 203–220.
[27] R. Renkiewicz, L. Qiu, C. Lesch, X. Sun, R. Devalaraja, T. Cody, E. Kaldjian, H. Welgus, V. Baragi, Broad-spectrum matrix metalloproteinase inhibitor Marimastat-induced musculoskeletal side effects in rats, Arthritis Rheum. 48 (2003) 1742–1749.
[28] A. Saghatelian, N. Jessani, A. Joseph, M. Humphrey, B.F. Cravatt, Activity-based probes for the proteomic profiling of metalloproteases, Proc. Natl. Acad. Sci. U. S. A. 101 (2004) 10000–10005.
[29] E. Candelario-Jalil, Y. Yang, G.A. Rosenberg, Diverse roles of matrix metalloproteinases and tissue inhibitors of metalloproteinases in neuroinflammation and cerebral ischemia, Neuroscience 158 (2009) 983–994.
[30] R.R. Sood, S. Taheri, E. Candelario-Jalil, E.Y. Estrada, G.A. Rosenberg, Early beneficial effect of matrix metalloproteinase inhibition on blood–brain barrier permeability as measured by magnetic resonance imaging countered by impaired long-term recovery after stroke in rat brain, J. Cereb. Blood Flow Metab. 28 (2008) 431–438.
[31] G.E. Terp, G. Cruciani, I.T. Christensen, F.S. Jorgensen, Structural differences of matrix metalloproteinases with potential implications for inhibitor selectivity examined by GRID/CPCA approach, J. Med. Chem. 45 (2002) 2675–2684.
[32] J.W. Skiles, N.C. Gonnella, A.Y. Jeng, The design, structure, and therapeutic application of matrix metalloproteinase inhibitors, Curr. Med. Chem. 8 (2001) 425–474.
[33] C.M. Overall, G.S. Butler, Protease yoga: extreme flexibility of a matrix metalloproteinase, Structure 15 (2007) 1159–1161.
[34] H. Tsukada, T. Pourmotabbed, Unexpected crucial role of residue 272 in substrate specificity of fibroblast collagenase, J. Biol. Chem. 277 (2002) 27378–27384.
[35] G. Velasco, A.M. Pendas, A. Fueyo, V. Knauper, G. Murphy, C. Lopez-Otin, Cloning and characterization of human MMP-23, a new matrix metalloproteinase predominantly expressed in reproductive tissues and lacking conserved domains in other family members, J. Biol. Chem. 274 (1999) 4570–4576.

[36] L. Aureli, M. Gioia, I. Cerbara, S. Monaco, G.F. Fasciglione, S. Marini, P. Ascenzi, A. Topai, M. Coletta, Structural bases for substrate and inhibitor recognition by matrix metalloproteinases, Curr. Med. Chem. 15 (2008) 2192–2222.
[37] I. Massova, L.P. Kotra, S. Mobashery, Structural insight into the binding motifs for the calcium ion and the non-catalytic zinc in matrix metalloproteases, Bioorganic Med. Chem. Lett. 8 (1998) 853–858.
[38] W. Bode, C. Fernandez-Catalana, H. Tscheschea, F. Grams, H. Nagasea, K. Maskos, Structural properties of matrix metalloproteinases, Cell. Mol. Life Sci. 55 (1999) 639–652.
[39] W. Bode, F.-X. Gomis-Ruth, W. Stockler, Astacins, serralysins, snake venom and matrix metalloproteinases exhibit identical zinc-binding environments (HEXXHXXGXXH and Met-turn) and topologies and should be grouped into a common family, the 'metzincins', Fed. Eur. Biochem. Soc. Lett. 331 (1993) 134–140.
[40] H.I. Park, Y. Jin, D.R. Hurst, C.A. Monroe, S. Lee, M.A. Schwartz, Q.-X.A. Sang, The intermediate S1' pocket of the endometase/matrilysin-2 active site revealed by enzyme inhibition kinetic studies, protein sequence analyses, and homology modeling, J. Biol. Chem. 278 (2003) 51646–51653.
[41] A.R. Johnson, A.G. Pavlovsky, D.F. Ortwine, F. Prior, C.-F. Man, D.A. Bornemeier, C.A. Banotai, W.T. Mueller, P. McConnell, C. Yan, V. Baragi, C. Lesch, W.H. Roark, M. Wilson, K. Datta, R. Guzman, H.-K. Han, R.D. Dyer, Discovery and characterization of a novel inhibitor of matrix metalloprotease-13 that reduces cartilage damage in vivo without joint fibroplasia side effects, J. Biol. Chem. 282 (2007) 27781–27791.
[42] A.-L. Gall, M. Ruff, R. Kannan, P. Cuniasse, A. Yiotakis, V. Dive, M.-C. Rio, P. Basset, D. Moras, Crystal structure of the stromelysin-3 (MMP-11) catalytic domain complexed with a phosphinic inhibitor mimicking the transition-state, J. Mol. Biol. 307 (2001) 577–586.
[43] M.F. Browner, W.W. Smith, A.L. Castelhano, Matrilysin–inhibitor complexes: common themes among metalloproteases, Biochemistry 34 (1995) 6602–6610.
[44] S. Netzelarnett, Q.X. Sang, W.G.I. Moore, M. Navre, H. Birkedalhansen, H.E. Vanwart, Comparative sequence specificities of human 72-Kda and 92-Kda gelatinases (type-IV collagenases) and pump (matrilysin), Biochemistry 32 (1993) 6427–6432.
[45] N. Borkakoti, F.K. Winkler, D.H. Williams, A. D'Arcy, M.J. Broadhurst, P.A. Brown, W.H. Johnson, E.J. Murray, Structure of the catalytic domain of human fibroblast collagenase complexed with an inhibitor, Nat. Struct. Biol. 1 (1994) 106–110.
[46] B. Lovejoy, A.R. Welch, S. Carr, C. Luong, C. Broka, R.T. Hendricks, J.A. Campbell, K. A.M. Walker, R. Martin, H. Van Wart, M.F. Browner, Crystal structures of MMP-1 and -13 reveal the structural basis for selectivity of collagenase inhibitors, Nat. Struct. Biol. 6 (1999) 217–221.
[47] M.R. Gowravaram, B.E. Tomczuk, J.S. Johnson, D. Delecki, E.R. Cook, A.K. Ghose, A.M. Mathiowetz, J.C. Spurlino, B. Rubin, D.L. Smith, T. Pulvino, R.C. Wahl, Inhibition of matrix metalloproteinases by hydroxamates containing heteroatom-based modifications of the P1' group, J. Med. Chem. 38 (1995) 2570–2581.
[48] J.W. Skiles, N.C. Gonnella, A.Y. Jeng, The design, structure, and clinical update of small molecular weight matrix metalloproteinase inhibitors, Curr. Med. Chem. 11 (2004) 2911–2977.
[49] S. Rowsell, P. Hawtin, C.A. Minshull, H. Jepson, S.M.V. Brockbank, D.G. Barratt, A.M. Slater, W.L. McPheat, D. Waterson, A.M. Henney, R.A. Pauptit, Crystal structure of human MMP9 in complex with a reverse hydroxamate inhibitor, J. Mol. Biol. 319 (2002) 173–181.
[50] A. Tochowicz, K. Maskos, R. Huber, R. Oltenfreiter, V. Dive, A. Yiotakis, M. Zanda, W. Bode, P. Goettig, Crystal structures of MMP-9 complexes with five inhibitors: contribution of the flexible Arg424 side-chain to selectivity, J. Mol. Biol. 371 (2007) 989–1006.
[51] E.I. Chen, W. Li, A. Godzik, E.W. Howard, J.W. Smith, A residue in the S2 subsite controls substrate selectivity of matrix metalloproteinase-2 and matrix metalloproteinase-9, J. Biol. Chem. 278 (2003) 17158–17163.
[52] B. Pirard, H. Matter, Matrix metalloproteinase target family landscape: a chemometrical approach to ligand selectivity based on protein binding site analysis, J. Med. Chem. 49 (2006) 51–69.
[53] H. Nar, K. Werle, M.M.T. Bauer, H. Dollinger, B. Jung, Crystal structure of human macrophage elastase (MMP-12) in complex with a hydroxamic acid inhibitor, J. Mol. Biol. 312 (2001) 743–751.
[54] X. Zhang, N.C. Gonnella, J. Koehn, N. Pathak, V. Ganu, R. Melton, D. Parker, S.-I. Hu, K.-Y. Nam, Solution structure of the catalytic domain of human collagenase-3 (MMP-13) complexed to a potent non-peptidic sulfonamide inhibitor: binding comparison with stromelysin-1 and collagenase-1, J. Mol. Biol. 301 (2000) 513–524.
[55] D.G. Hangauer, A.F. Monzingo, B.W. Matthews, An interactive computer graphics study of thermolysin-catalyzed peptide cleavage and inhibition by *N*-carboxymethyl dipeptides, Biochemistry 23 (1984) 5730–5741.
[56] B.W. Matthews, Structural basis of the action of thermolysin and related zinc peptidases, Acc. Chem. Res. 21 (1988) 333–340.
[57] B. Lovejoy, A.M. Hassell, M.A. Luther, D. Weigl, S.R. Jordan, Crystal structures of recombinant 19-kDa human fibroblast collagenase complexed to itself, Biochemistry 33 (1994) 8207–8217.
[58] S.P. Gupta, Quantitative structure–activity relationship studies on zinc-containing metalloproteinase inhibitors, Chem. Rev. 107 (2007) 3042–3087.
[59] G. Elaut, V. Rogiers, T. Vanhaecke, The pharmaceutical potential of histone deactylase inhibitors, Curr. Pharm. Des. 13 (2007) 2584–2620.
[60] M.L. Moss, L. Sklair-Tavron, R. Nudelman, Drug insight: Tumor necrosis factor-converting enzyme as a pharmaceutical target for rheumatoid arthritis, Nat. Clin. Pract. Rheumat. 4 (2008) 300–309.
[61] R.J. Cherney, R. Mo, D.T. Meyer, K.D. Hardman, R.-Q. Liu, M.B. Covington, M. Qian, Z.R. Wasserman, D.D. Christ, J.M. Trzaskos, R.C. Newton, C.P. Decicco, Sultam hydroxamates as novel matrix metalloproteinase inhibitors, J. Med. Chem. 47 (2004) 2981–2983.
[62] S. Nakatani, M. Ikura, S. Yamamoto, Y. Nishita, S. Itadani, H. Habashita, T. Sugiura, K. Ogawa, H. Ohno, K. Takahashi, H. Nakai, M. Toda, Design and synthesis of novel metalloproteinase inhibitors, Bioorganic Med. Chem. 14 (2006) 5402–5422.
[63] A. Rossello, E. Nuti, P. Carelli, E. Orlandini, M. Macchia, S. Nencetti, M. Zandomeneghi, F. Balzano, G.U. Barretta, A. Albini, R. Benelli, G. Cercignani, G. Murphy, A. Balsamo, *N*-*i*-Propoxy-*N*-biphenylsulfonylaminobutylhydroxamic acids as potent and selective inhibitors of MMP-2 and MT1-MMP, Bioorganic Med. Chem. Lett. 15 (2005) 1321–1326.
[64] R. Subramaniam, M.K. Haldar, S. Tobwala, B. Ganguly, D.K. Srivastava, S. Mallik, Novel bis-(arylsulfonamide) hydroxamate-based selective MMP inhibitors, Bioorganic Med. Chem. Lett. 18 (2008) 3333–3337.
[65] G.A. Whitlock, K.N. Dack, R.P. Dickinson, M.L. Lewis, A novel series of highly selective inhibitors of MMP-3, Bioorganic Med. Chem. Lett. 17 (2007) 6750–6753.
[66] F.E. Jacobsen, M.W. Buczynski, E.A. Dennis, S.M. Cohen, A macrophage cell model for selective metalloproteinase inhibitor design, ChemBioChem 9 (2008) 2087–2095.
[67] A.O. Stewart, P.A. Bhatia, J.G. Martin, J.B. Summers, K.E. Rodriques, M.B. Martin, J.H. Holms, J.L. Moore, R.A. Craig, T. Kolasa, J.D. Ratajczyk, H. Mazdiyasni, F.A.J. Kerdesky, S.L. DeNinno, R.G. Maki, J.B. Bouska, P.R. Young, C. Lanni, R.L. Bell, G.W. Carter, C.D.W. Brooks, Structure–activity relationships of *N*-hydroxyurea 5-lipoxygenase inhibitors, J. Med. Chem. 40 (1997) 1955–1968.
[68] Y. Hu, J.S. Xiang, M.J. DiGrandi, X. Du, M. Ipek, L.M. Laakso, J. Li, W. Li, T.S. Rush, J. Schmid, J.S. Skotnicki, S. Tam, J.R. Thomason, Q. Wang, J.I. Levin, Potent, selective, and orally bioavailable matrix metalloproteinase-13 inhibitors for the treatment of osteoarthritis, Bioorganic Med. Chem. 13 (2005) 6629–6644.
[69] J. Li, T.S. Rush III, W. Li, D. DeVincentis, X. Du, Y. Hu, J.R. Thomason, J.S. Xiang, J.S. Skotnicki, S. Tam, K.M. Cunningham, P.S. Chockalingam, E.A. Morris, J.I. Levin, Synthesis and SAR of highly selective MMP-13 inhibitors, Bioorganic Med. Chem. Lett. 15 (2005) 4961–4966.
[70] J. Wu, T.S. Rush III, R. Hotchandani, X. Du, M. Geck, E. Collins, Z.-B. Xu, J. Skotnicki, J.I. Levin, F.E. Lovering, Identification of potent and selective MMP-13 inhibitors, Bioorganic Med. Chem. Lett. 15 (2005) 4105–4109.
[71] W. Li, J. Li, Y. Wu, J. Wu, R. Hotchandani, K. Cunningham, I. McFadyen, J. Bard, P. Morgan, F. Schlerman, X. Xu, S. Tam, S.J. Goldman, C. Williams, J. Sypek, T.S. Mansour, A selective matrix metalloprotease 12 inhibitor for potential treatment of chronic obstructive pulmonary disease (COPD): discovery of (*S*)-2-(8-(methoxycarbonylamino)dibenzo[*b*,*d*]furan- 3-sulfonamido)-3-methylbutanoic acid (MMP408), J. Med. Chem. 52 (2009) 1799–1802.
[72] D.T. Puerta, J.A. Lewis, S.M. Cohen, New beginnings for matrix metalloproteinase inhibitors: identification of high-affinity zinc-binding groups, J. Am. Chem. Soc. 126 (2004) 8388–8389.
[73] D.T. Puerta, M.O. Griffin, J.A. Lewis, D. Romero-Perez, R. Garcia, F.J. Villarreal, S.M. Cohen, Heterocyclic zinc-binding groups for use in next-generation matrix metalloproteinase inhibitors: potency, toxicity, and reactivity, J. Biol. Inorg. Chem. 11 (2006) 131–138.
[74] J.A. Lewis, J. Mongan, J.A. McCammon, S.M. Cohen, Evaluation and binding-mode prediction of thiopyrone-based inhibitors of anthrax lethal factor, ChemMedChem 1 (2006) 694–697.
[75] A. Agrawal, D. Romero-Perez, J.A. Jacobsen, F.J. Villarreal, S.M. Cohen, Zinc-binding groups modulate selective inhibition of MMPs, ChemMedChem 3 (2008) 812–820.
[76] D.T. Puerta, J. Mongan, B.L. Tran, J.A. McCammon, S.M. Cohen, Potent, selective pyrone-based inhibitors of stromelysin-1, J. Am. Chem. Soc. 127 (2005) 14148–14149.
[77] Y.-M. Zhang, X. Fan, D. Chakaravarty, B. Xiang, R.H. Scannevin, Z. Huang, J. Ma, S.L. Burke, P. Karnachi, K.J. Rhodes, P.F. Jackson, 1-Hydroxy-2-pyridinone-based MMP inhibitors: synthesis and biological evaluation for the treatment of ischemic stroke, Bioorganic Med. Chem. Lett. 18 (2008) 409–413.
[78] Y.-M. Zhang, X. Fan, S.-M. Yang, R.H. Scannevin, S.L. Burke, K.J. Rhodes, P.F. Jackson, Syntheses and in vitro evaluation of arylsulfone-based MMP inhibitors with heterocycle-derived zinc-binding groups (ZBGs), Bioorganic Med. Chem. Lett. 18 (2008) 405–408.
[79] F. Auge, W. Hornebeck, M. Decarme, J.-Y. Laronze, Improved gelatinase A selectivity by novel zinc binding groups containing galardin derivatives, Bioorganic Med. Chem. Lett. 13 (2003) 1783–1786.
[80] G. LeDour, G. Moroy, M. Rouffet, E. Bourguet, D. Guillaume, M. Decarme, H. ElMourabit, F. Augé, A.J.P. Alix, J.-Y. Laronze, G. Bellon, W. Hornebeck, J. Sapi, Introduction of the 4-(4-bromophenyl)benzenesulfonyl group to hydrazide analogs of Ilomastat leads to potent gelatinase B (MMP-9) inhibitors with improved selectivity, Bioorganic Med. Chem. 16 (2008) 8745–8759.
[81] M.R. Michaelides, J.F. Dellaria, J. Gong, J.H. Holms, J.J. Bouska, J. Stacey, C.K. Wada, H.R. Heyman, M.L. Curtin, Y. Guo, C.L. Goodfellow, I.B. Elmore, D.H. Albert, T.J. Magoc, P.A. Marcotte, D.W. Morgan, S.K. Davidsen, Biaryl ether retrohydroxamates as potent, long-lived, orally bioavailable MMP inhibitors, Bioorganic Med. Chem. Lett. 11 (2001) 1553–1556.
[82] C. Campestre, M. Agamennone, P. Tortorella, S. Preziuso, A. Biasone, E. Gavuzzo, G. Pochetti, F. Mazza, O. Hiller, H. Tschesche, V. Consalvi, C. Gallina, *N*-Hydroxyurea as zinc binding group in matrix metalloproteinase inhibition: mode of binding in a complex with MMP-8, Bioorganic Med. Chem. Lett. 16 (2006) 20–24.

[83] B.B. Nielsen, K. Frydenvang, I.K. Larsen, Structures of two ribonucleotide reductase inhibitors: 1-hydroxy-1-methylurea and 1-hydroxy-3-methylurea, Acta Crystallogr., Sec. C 49 (1993) 1018–1022.
[84] M.B. Onaran, A.B. Comeau, C.T. Seto, Squaric acid-based peptidic inhibitors of matrix metalloprotease-1, J. Org. Chem. 70 (2005) 10792–10802.
[85] D.R. Hurst, M.A. Schwartz, Y. Jin, M.A. Ghaffari, P. Kozarekar, J. Cao, Q.-X.A. Sang, Inhibition of enzyme activity of and cell-mediated substrate cleavage by membrane type 1 matrix metalloproteinase by newly developed mercaptosulphide inhibitors, Biochem. J. 392 (2005) 527–536.
[86] H. Nakahara, L. Howard, E.W. Thompson, H. Sato, M. Seiki, Y. Yeh, W.-T. Chen, Transmembrane/cytoplasmic domain-mediated membrane type 1-matrix metalloprotease docking to invadopodia is required for cell invasion, Proc. Natl. Acad. Sci. U. S. A. 94 (1997) 7959–7964.
[87] G. Pochetti, E. Gavuzzo, C. Campestre, M. Agamennone, P. Tortorella, V. Consalvi, C. Gallina, O. Hiller, H. Tschesche, P.A. Tucker, F. Mazza, Structural insight into the stereoselective inhibition of MMP-8 by enantiomeric sulfonamide phosphonates, J. Med. Chem. 49 (2006) 923–931.
[88] A. Biasone, P. Tortorella, C. Campestre, M. Agamennone, S. Preziuso, M. Chiappini, E. Nuti, P. Carelli, A. Rossello, F. Mazza, C. Gallina, Alpha-biphenylsulfonylamino 2-methylpropyl phosphonates: enantioselective synthesis and selective inhibition of MMPs, Bioorganic Med. Chem. 15 (2007) 791–799.
[89] P.M. O'Brien, D.F. Ortwine, A.G. Pavlovsky, J.A. Picard, D.R. Sliskovic, B.D. Roth, R.D. Dyer, L.L. Johnson, C.F. Man, H. Hallak, Structure–activity relationships and pharmacokinetic analysis for a series of potent, systemically available biphenylsulfonamide matrix metalloproteinase inhibitors, J. Med. Chem. 43 (2000) 156–166.
[90] A.R. Folgueras, A. Fueyo, O. Garcia-Suarez, J. Cox, A. Astudillo, P. Tortorella, C. Campestre, A. Gutierrez-Fernandez, M. Fanjul-Fernandez, C.J. Pennington, D.R. Edwards, C.M. Overall, C. Lopez-Otin, Collagenase-2 deficiency or inhibition impairs experimental autoimmune encephalomyelitis in mice, J. Biol. Chem. 283 (2008) 9465–9474.
[91] P. Van Lint, B. Wielockx, L. Puimege, A. Noel, C. Lopez-Otin, C. Libert, Resistance of collagenase-2 (matrix metalloproteinase-8)-deficient mice to TNF-induced lethal hepatitis, J. Immunol. 175 (2005) 7642–7649.
[92] M. Matziari, F. Beau, P. Cuniasse, V. Dive, A. Yiotakis, Evaluation of P1'-diversified phosphinic peptides leads to the development of highly selective inhibitors of MMP-11, J. Med. Chem. 47 (2004) 325–336.
[93] E. Farkas, Y. Katz, S. Bhusare, R. Reich, G.-V. Roschenthaler, M. Konigsmann, E. Breuer, Carbamoylphosphonate-based matrix metalloproteinase inhibitor metal complexes: solution studies and stability constants. Towards a zinc-selective binding group, J. Biol. Inorg. Chem. 9 (2004) 307–315.
[94] E. Breuer, C.J. Salomon, Y. Katz, W. Chen, S. Lu, G.-V. Roschenthaler, R. Hadar, R. Reich, Carbamoylphosphonates, a new class of in vivo active matrix metalloproteinase inhibitors. 1. Alkyl- and cycloalkylcarbamoylphosphonic acids, J. Med. Chem. 47 (2004) 2826–2832.
[95] A. Hoffman, B. Qadri, J. Frant, Y. Katz, S.R. Bhusare, E. Breuer, R. Hadar, R. Reich, Carbamoylphosphonate matrix metalloproteinase inhibitors 6: *cis*-2-aminocyclohexylcarbamoylphosphonic acid, a novel orally active antimetastatic matrix metalloproteinase-2 selective inhibitor—synthesis and pharmacodynamic and pharmacokinetic analysis, J. Med. Chem. 51 (2008) 1406–1414.
[96] F.E. Jacobsen, J.A. Lewis, S.M. Cohen, A new role for old ligands: discerning chelators for zinc metalloproteinases, J. Am. Chem. Soc. 128 (2006) 3156–3157.
[97] G.R. Cook, E. Manivannan, T. Underdahl, V. Lukacova, Y. Zhang, S. Balaz, Synthesis and evaluation of novel oxazoline MMP inhibitors, Bioorganic Med. Chem. Lett. 14 (2004) 4935–4939.
[98] F. Grams, H. Brandstetter, S. D'Alò, D. Geppert, H.-W. Krell, H. Leinert, V. Livi, E. Menta, A. Oliva, G. Zimmermann, Pyrimidine-2,4,6-triones: a new effective and selective class of matrix metalloproteinasae inhibitors, Biol. Chem. 382 (2001) 1277–1285.
[99] H. Brandstetter, F. Grams, D. Glitz, A. Lang, R. Huber, W. Bode, H.-W. Krell, R.A. Engh, The 1.8-Å crystal structure of a matrix metalloproteinase 8-barbiturate inhibitor complex reveals a previously unobserved mechanism for collagenase substrate recognition, J. Biol. Chem. 276 (2001) 17405–17412.
[100] L.H. Foley, R. Palermo, P. Dunten, P. Wang, Novel 5,5-disubstitutedpyrimidine-2,4,6-triones as selective MMP inhibitors, Bioorganic Med. Chem. Lett. 11 (2001) 969–972.
[101] P. Dunten, U. Kammlott, R. Crowther, W. Levin, L.H. Foley, P. Wang, R. Palermo, X-ray structure of a novel matrix metalloproteinase inhibitor complexed to stromelysin, Protein Sci. 10 (2001) 923–926.
[102] E. Maquoi, N.E. Sounni, L. Devy, F. Olivier, F. Frankenne, H.-W. Krell, F. Grams, J.-M. Foidart, A. Noel, Anti-invasive, antitumoral, and antiangiogenic efficacy of a pyrimidine-2,4,6-trione derivative, an orally active and selective matrix metalloproteinases inhibitor, Clin. Cancer Res. 10 (2004) 4038–4047.
[103] S.-H. Kim, A.T. Pudzianowski, K.J. Leavitt, J. Barbosa, P.A. McDonnell, W.J. Metzler, B.M. Rankin, R. Liu, W. Vaccaro, W. Pitts, Structure-based design of potent and selective inhibitors of collagenase-3 (MMP-13), Bioorganic Med. Chem. Lett. 15 (2005) 1101–1106.
[104] J.A. Blagg, M.C. Noe, L.A. Wolf-Gouveia, L.A. Reiter, E.R. Laird, S.-P.P. Chang, D.E. Danley, J.T. Downs, N.C. Elliott, J.D. Eskra, R.J. Griffiths, J.R. Hardink, A.I. Haugeto, C.S. Jones, J.L. Liras, L.L. Lopresti-Morrow, P.G. Mitchell, J. Pandit, R.P. Robinson, C. Subramanyam, M.L. Vaughn-Bowser, S.A. Yocum, Potent pyrimidinetrione-based inhibitors of MMP-13 with enhanced selectivity over MMP-14, Bioorganic Med. Chem. Lett. 15 (2005) 1807–1810.
[105] L.A. Reiter, K.D. Freeman-Cook, C.S. Jones, G.J. Martinelli, A.S. Antipas, M.A. Berliner, K. Datta, J.T. Downs, J.D. Eskra, M.D. Forman, E.M. Greer, R. Guzman, J.R. Hardink, F. Janat, N.F. Keene, E.R. Laird, J.L. Liras, L.L. Lopresti-Morrow, P.G. Mitchell, J. Pandit, D. Robertson, D. Sperger, M.L. Vaughn-Bowser, D.M. Waller, S.A. Yocum, Potent, selective pyrimidinetrione-based inhibitors of MMP-13, Bioorganic Med. Chem. Lett. 16 (2006) 5822–5826.
[106] K.D. Freeman-Cook, L.A. Reiter, M.C. Noe, A.S. Antipas, D.E. Danley, K. Datta, J.T. Downs, S. Eisenbeis, J.D. Eskra, D.J. Garmene, E.M. Greer, R.J. Griffiths, R. Guzman, J.R. Hardink, F. Janat, C.S. Jones, G.J. Martinelli, P.G. Mitchell, E.R. Laird, J.L. Liras, L. L. Lopresti-Morrow, J. Pandit, U.D. Reilly, D. Robertson, M.L. Vaughn-Bowser, L.A. Wolf-Gouviea, S.A. Yocum, Potent, selective spiropyrrolidine pyrimidinetrione inhibitors of MMP-13, Bioorganic Med. Chem. Lett. 17 (2007) 6529–6534.
[107] D.T. Puerta, S.M. Cohen, Examination of novel zinc-binding groups for use in matrix metalloproteinase inhibitors, Inorg. Chem. 42 (2003) 3423–3430.
[108] F.E. Jacobsen, J.A. Lewis, K.J. Heroux, S.M. Cohen, Characterization and evaluation of pyrone and tropolone chelators for use in metalloprotein inhibitors, Inorg. Chim. Acta 360 (2007) 264–272.
[109] Y.-L. Yan, S.M. Cohen, Efficient synthesis of 5-amido-3-hydroxy-4-pyrones as inhibitors of matrix metalloproteinases, Org. Lett. 9 (2007) 2517–2520.
[110] J.J. Li, J. Nahra, A.R. Johnson, A. Bunker, P. O'Brien, W.-S. Yue, D.F. Ortwine, C.-F. Man, V. Baragi, K. Kilgore, R.D. Dyer, H.-K. Han, Quinazolinones and pyrido[3,4-*d*]pyrimidin-4-ones as orally active and specific matrix metalloproteinase-13 inhibitors for the treatment of osteoarthritis, J. Med. Chem. 51 (2008) 835–841.
[111] R. Morales, S. Perrier, J.-M. Florent, J. Beltra, S. Dufour, I. De Mendez, P. Manceau, A. Tertre, F. Moreau, D. Compere, A.-C. Dublanchet, M. O'Gara, Crystal structures of novel non-peptidic, non-zinc chelating inhibitors bound to MMP-12, J. Mol. Biol. 341 (2004) 1063–1076.
[112] C.K. Engel, B. Pirard, S. Schimanski, R. Kirsch, J. Habermann, O. Klingler, V. Schlotte, K.U. Weithmann, K.U. Wendt, Structural basis for the highly selective inhibition of MMP-13, Chem. Biol. 12 (2005) 181–189.
[113] A.-C. Dublanchet, P. Ducrot, C. Andrianjara, M. O'Gara, R. Morales, D. Compere, A. Denis, S. Blais, P. Cluzeau, K. Courte, J. Hamon, F. Moreau, M.-L. Prunet, A. Tertre, Structure-based design and synthesis of novel non-zinc chelating MMP-12 inhibitors, Bioorganic Med. Chem. Lett. 15 (2005) 3787–3790.
[114] J.M. Chen, F.C. Nelson, J.I. Levin, D. Mobilio, F.J. Moy, R. Nilakantan, A. Zask, R. Powers, Structure-based design of a novel, potent, and selective inhibitor for MMP-13 utilizing NMR spectroscopy and computer-aided molecular design, J. Am. Chem. Soc. 122 (2000) 9648–9654.
[115] L.T. Gooljarsingh, A. Lakdawala, F. Coppo, L. Luo, G.B. Fields, P.J. Tummino, R.R. Gontarek, Characterization of an exosite binding inhibitor of matrix metalloproteinase 13, Protein Sci. 17 (2008) 66–71.
[116] G. Pochetti, R. Montanari, C. Gege, C. Chevrier, A.G. Taveras, F. Mazza, Extra binding region induced by non-zinc chelating inhibitors into the S1' subsite of matrix metalloproteinase 8 (MMP-8), J. Med. Chem. 52 (2009) 1040–1049.
[117] S. Brown, M.M. Bernardo, Z.-H. Li, L.P. Kotra, Y. Tanaka, R. Fridman, S. Mobashery, Potent and selective mechanism-based inhibition of gelatinases, J. Am. Chem. Soc. 122 (2000) 6799–6800.
[118] D.P. Becker, C.I. Villamil, T.E. Barta, L.J. Bedell, T.L. Boehm, G.A. DeCrescenzo, J.N. Freskos, D.P. Getman, S. Hockerman, R. Heintz, S.C. Howard, M.H. Li, J.J. McDonald, C.P. Carron, C.L. Funckes-Shippy, P.P. Mehta, G.E. Munie, C.A. Swearingen, Synthesis and structure–activity relationships of beta- and alpha-piperidine sulfone hydroxamic acid matrix metalloproteinase inhibitors with oral antitumor efficacy, J. Med. Chem. 48 (2005) 6713–6730.
[119] J.N. Freskos, J.J. McDonald, B.V. Mischke, P.B. Mullins, H.-S. Shieh, R.A. Stegeman, A.M. Stevens, Synthesis and identification of conformationally constrained selective MMP inhibitors, Bioorganic Med. Chem. Lett. 9 (1999) 1757–1760.
[120] J.N. Freskos, B.V. Mischke, G.A. DeCrescenzo, R. Heintz, D.P. Getman, S.C. Howard, N.N. Kishore, J.J. McDonald, G.E. Munie, S. Rangwala, C.A. Swearingen, C. Voliva, D.J. Welsch, Discovery of a novel series of selective MMP inhibitors: identification of the gamma-sulfone-thiols, Bioorganic Med. Chem. Lett. 9 (1999) 943–948.
[121] H. Moriyama, T. Tsukida, Y. Inoue, K. Yokota, K. Yoshino, H. Kondo, N. Miura, S.-I. Nishimura, Azasugar-based MMP/ADAM inhibitors as antipsoriatic agents, J. Med. Chem. 47 (2004) 1930–1938.
[122] L.A. Reiter, R.P. Robinson, K.F. McClure, C.S. Jones, M.R. Reese, P.G. Mitchell, I.G. Otterness, M.L. Bliven, J. Liras, S.R. Cortina, K.M. Donahue, J.D. Eskra, R.J. Griffiths, M.E. Lame, A. Lopez-Anaya, G.J. Martinelli, S.M. McGahee, S.A. Yocum, L.L. Lopresti-Morrow, L.M. Tobiassen, M.L. Vaughn-Bowser, Pyran-containing sulfonamide hydroxamic acids: potent MMP inhibitors that spare MMP-1, Bioorganic Med. Chem. Lett. 14 (2004) 3389–3395.
[123] S. Yamamoto, S. Nakatani, M. Ikura, T. Sugiura, Y. Nishita, S. Itadani, K. Ogawa, H. Ohno, K. Takahashi, H. Nakai, M. Toda, Design and synthesis of an orally active matrix metalloproteinase inhibitor, Bioorganic Med. Chem. 14 (2006) 6383–6403.
[124] S.-M. Yang, R.H. Scannevin, B. Wang, S.L. Burke, L.J. Wilson, P. Karnachi, K.J. Rhodes, B. Lagu, W.V. Murray, Beta-*N*-biaryl ether sulfonamide hydroxamates as potent gelatinase inhibitors. Part 1. Design, synthesis, and lead identification, Bioorganic Med. Chem. Lett. 18 (2008) 1135–1139.
[125] O. Kleifeld, L.P. Kotra, D.C. Gervasi, S. Brown, M.M. Bernardo, R. Fridman, S. Mobashery, I. Sagi, X-ray absorption studies of human matrix metalloproteinase-2 (MMP-2) bound to a highly selective mechanism-based inhibitor, J. Biol. Chem. 276 (2001) 17125–17131.
[126] J.F. Morrison, C.T. Walsh, The behavior and significance of slow-binding enzyme inhibitors, Advan. Enzymol. Relat. Areas Mol. Biol. 61 (1988) 201–301.
[127] G. Rosenblum, S.O. Meroueh, O. Kleifeld, S. Brown, S.P. Singson, R. Fridman, S. Mobashery, I. Sagi, Structural basis for potent slow binding inhibition of human matrix metalloproteinase-2 (MMP-2), J. Biol. Chem. 278 (2003) 27009–27015.

[128] M. Lee, M.M. Bernardo, S.O. Meroueh, S. Brown, R. Fridman, S. Mobashery, Synthesis of chiral 2-(4-phenoxyphenylsulfonylmethyl)thiiranes as selective gelatinase inhibitors, Org. Lett. 7 (2005) 4463–4465.
[129] M. Toth, M.M. Bernardo, D.C. Gervasi, P.D. Soloway, Z. Wang, H.F. Bigg, C.M. Overall, Y.A. DeClerck, H. Tschesche, M.L. Cher, S. Brown, S. Mobashery, R. Fridman, Tissue inhibitor of metalloproteinase (TIMP)-2 acts synergistically with synthetic matrix metalloproteinase (MMP) inhibitors but not with TIMP-4 to enhance the (membrane type 1)-MMP-dependent activation of pro-MMP-2, J. Biol. Chem. 275 (2000) 41415–41423.
[130] M. Ikejiri, M.M. Bernardo, R.D. Bonfil, M. Toth, M. Chang, R. Fridman, S. Mobashery, Potent mechanism-based inhibitors for matrix metalloproteinases, J. Biol. Chem. 280 (2005) 33992–34002.
[131] M.M. Bernardo, S. Brown, Z.-H. Li, R. Fridman, S. Mobashery, Design, synthesis, and characterization of potent, slow-binding inhibitors that are selective for gelatinases, J. Biol. Chem. 277 (2002) 11201–11207.
[132] A. Kruger, M.J.E. Arlt, M. Gerg, C. Kopitz, M.M. Bernardo, M. Chang, S. Mobashery, R. Fridman, Antimetastatic activity of a novel mechanism-based gelatinase inhibitor, Cancer Res. 65 (2005) 3523–3526.
[133] R.D. Bonfil, A. Sabbota, S. Nabha, M.M. Bernardo, Z. Dong, H. Meng, H. Yamamoto, S.R. Chinni, I.T. Lim, M. Chang, L.C. Filetti, S. Mobashery, M.L. Cher, R. Fridman, Inhibition of human prostate cancer growth, osteolysis and angiogenesis in a bone metastasis model by a novel mechanism-based selective gelatinase inhibitor, Int. J. Cancer 118 (2006) 2721–2726.
[134] R.D. Bonfil, Z. Dong, J.C.T. Filho, A. Sabbota, P. Osenkowski, S. Nabha, H. Yamamoto, S.R. Chinni, H. Zhao, S. Mobashery, R.L. Vessella, R. Fridman, M.L. Cher, Prostate cancer-associated membrane type 1-matrix metalloproteinase, Am. J. Pathol. 170 (2007) 2100–2111.
[135] A. Kruger, R. Soeltl, I. Sopov, C. Kopitz, M. Arlt, V. Magdolen, N. Harbeck, B. Gansbacher, M. Schmitt, Hydroxamate-type matrix metalloproteinase inhibitor Batimastat promotes liver metastasis, Cancer Res. 61 (2001) 1272–1275.
[136] Z. Gu, J. Cui, S. Brown, R. Fridman, S. Mobashery, A.Y. Strongin, S.A. Lipton, A highly specific inhibitor of matrix metalloproteinase-9 rescues laminin from proteolysis and neurons from apoptosis in transient focal cerebral ischemia, J. Neurosci. 25 (2005) 6401–6408.
[137] M. Lee, A. Villegas-Estrada, G. Celenza, B. Boggess, M. Toth, G. Kreitinger, C. Forbes, R. Fridman, S. Mobashery, M. Chang, Metabolism of a highly selective gelatinase inhbitor generates active metabolite, Chem. Biol. Drug Des. 70 (2007) 371–382.
[138] G. Celenza, A. Villegas-Estrada, M. Lee, B. Boggess, C. Forbes, W.R. Wolter, M.A. Suckow, S. Mobashery, M. Chang, Metabolism of (4-phenoxyphenylsulfonyl) methylthiirane, a selective gelatinase inhibitor, Chem. Biol. Drug Des. 71 (2008) 187–196.
[139] M. Lee, G. Celenza, B. Boggess, J. Blase, Q. Shi, M. Toth, M.M. Bernardo, W.R. Wolter, M.A. Suckow, D. Hesek, B.C. Noll, R. Fridman, S. Mobashery, M. Chang, A potent gelatinase inhibitor with anti-tumor-invasive activity and its metabolic disposition, Chem. Biol. Drug Des. 73 (2009) 189–202.
[140] J.B. Cross, J.S. Duca, J.J. Kaminski, V.S. Madison, The active site of a zinc-dependent metalloproteinase influences the computed pK(a) of ligands coordinated to the catalytic zinc ion, J. Am. Chem. Soc. 124 (2002) 11004–11007.
[141] I. Botos, L. Scapozza, D. Zhang, L.A. Liotta, E.F. Meyer, Batimastat, a potent matrix metalloproteinase inhibitor, exhibits an unexpected mode of binding, Proc. Natl. Acad. Sci. U. S. A. 93 (1996) 2749–2754.